Control of Wave Energy Converters in arrays

Simon Thomas

UPPSALA
UNIVERSITET

Abstract

One way to lower the levelized cost of energy for wave power plants and paving so the way for commercial success, is to increase the power absorption by use of advanced control algorithms. This thesis investigates the influence of the generator inertia, the generator damping and the layout on power absorption and presents a new model free strategy of controlling wave energy converters.

The evaluation of all control strategies was done in a numerical simulation and in experimental 1:10 model scale wave tank tests conducted in the COAST laboratory at the University of Plymouth. The WECs used are inspired by the wave energy concept developed at Uppsala University.

The influence of the generator inertia on the power absorption was tested with an uncontrolled WEC. Compared to a conventional WEC the power output could be significantly increased for small waves and high wave periods.

As a simple and easy to implement a control strategy, a WEC with sea state optimized generator damping was used to create a power matrix. The optimal damping factor depends on both wave period and wave height. The power absorption increases with the wave height and when the wave period converges towards the oscillation period of the WEC.

A genetic algorithm was used to obtain the optimized layouts for wave energy farms, which suggest that the converter should be placed in rows parallel to the wave front, and the position in the array has almost no influence on the optimal control parameter.

Finally, a collaborative learning approach using machine learning is presented, with several identical wave energy converters in a row to parallelise the search of the optimal control parameter. It was implemented to control the generator damping factor and the latching time. With the latter the power could be increased significantly.

List of papers

This thesis is based on the following papers, which are referred to in the text by their Roman numerals.

I **Thomas, S.**, Giassi, M., Göteman, M., Hann, M., Ransley, E., Isberg, J., Engström, J., "Performance of a Direct-Driven Wave Energy Point Absorber with High Inertia Rotatory Power Take-off", Energies, 2018, 11, 2332, Basel, Switzerland, doi: 10.3390/en11092332

II **Thomas, S.**, Giassi, M., Göteman, M., Ericsson, M., Isberg, J, Engström, J., "Optimal Constant Damping Control of a Point Absorber with Linear Generator In Different Sea States: Comparison of Simulation and Scale Test", Proceedings of the 12th European Wave and Tidal Energy Conference 2017, Cork, Ireland

III Giassi, M., Göteman, M., **Thomas, S.**, Engström, J., Eriksson, M., Isberg, J., "Multi-parameter optimization of hybrid arrays point absorber Wave Energy Converters", Proceedings of the 12th European Wave and Tidal Energy Conference 2017, Cork, Ireland

IV **Thomas, S.**, Giassi, M., Eriksson, M., Göteman, M., Ransley, E., Hann, M., Isberg, Jan., Engström, J., "A model free control based on machine learning for energy converters in an array", Submitted to Big Data And Cognitive Computing, 2018

V **Thomas, S.**, Göteman, M., Isberg, J., Eriksson, M., Ransley, E., Hann, M., Engström, J., "Experimental and numerical collaborative latching control of wave energy converter arrays", accepted for publication in Energies, 2018

Contents

Abbreviations

Abbreviation	Description
ANN	artificial neural network
BEM	boundary element method
CL	collaborative learning
COAST laboratory	coastal, ocean and sediment transport laboratory; Facility at the University of Plymouth containing the wave tank
cWEC	WEC with constant damping factor or latching time
g	gravity acceleration
lWEC	learnable WEC
PTO	power take off
WAMIT	WaveAnalysisMIT; Wave-body interaction analysing tool
WEC	wave energy converter

1. Introduction

For seamen like James Cook the energy transported in ocean waves was mostly seen as a danger which should be avoided. But when he landed with his ship HMS Endeavour in Tahiti in 1769, he could observe people bathing in the water, enjoying the waves and trying to ride them. Maybe this was the first time wave energy was used for human purposes.

Over two-hundred years later some people still like to ride waves, but much more they enjoy the comfort of nowadays electrical powered world and also here wave energy could be useful. To ensure a sustainable electrical energy supply in the future, electrical energy converted from ocean waves may play an important role. However, despite a long history of research in wave energy conversation and a wide range of proposed wave energy converter (WEC) designs, the idea, as easy and reasonable it seems, is not brought to a commercial scale yet.

For commercial success the levelized cost of energy have to be at or below the level of other electricity plants, what is not the case for WECs yet. To lower these costs, the cost of each WEC has to be reduced, for example by simplified designs or the power production has to be increased, for example by using advanced control strategies. As the energy density of ocean waves is much lower than for fossil fuels, most wave energy converter produces much less power than a conventional power plant. To produce significant amounts of energy WECs have to be put into farms consisting of ten to thousands of WECs, which brings new challenges how to place the devices and how to control them.

The history of modern wave energy research dates back to the 1970s and since then a wide range of concepts for wave energy converter were developed [1]. However, due to the way WECs interact with the waves, these designs can be classified in three categories: attenuators, terminators and absorbers. The latter is especially popular as point absorber, where a buoy that is small compared to the wave length, absorbs the energy.

1.1 Wave energy research at Uppsala University

The wave energy research at Uppsala University dates back to the beginning of this century [2], when a generator concept was developed [3], and later built an tested in full scale [4] close to Lysekil at the west coast of Sweden, what became the test site for several wave energy prototypes [5, 6, 7, 8]. The research

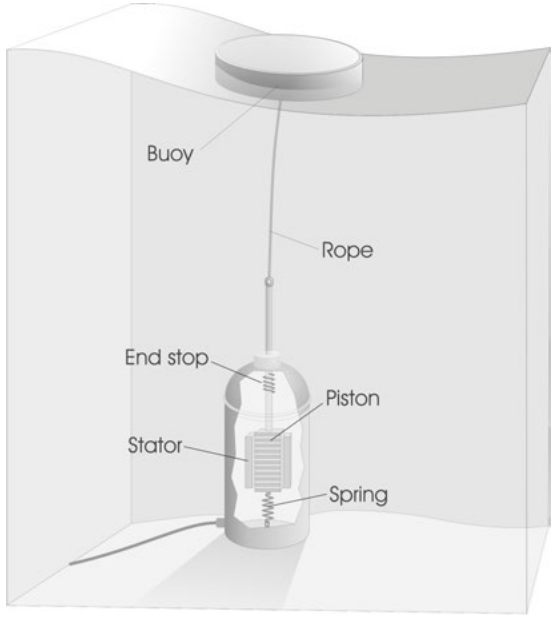

Figure 1.1. Sketch of the wave energy converter concept developed at Uppsala university.

focuses on nearly all aspects of wave energy, from the WEC design [9, 10] and deployment [11], the sensor system [12, 13] and grid connection [14], but also the control of WECs [15, 16], the survivability in extreme waves [17], the interaction in wave energy farms [18], the deployment and maintenance with help of remotely operated underwater vehicles [19] as well as environmental aspects [20]. The WEC's installed at the Lysekil testsite, in this thesis refered as UU-WEC, are floating point absorbers of the heave buoy type with gravity mounted direct-driven three-phase linear generators at the seabed. Generator and buoy are connected with a line. End stops spring inside the generator housing prevent the translator damaging the generator when pulled further than the stroke length. See Figure 1.1 for a sketch of the WEC. The generators are connected to a substation that is connected to a control centre on the main land, where it can be either connected to the grid or to a load resistance. By changing the load resistance, the generator damping can be controlled.

1.2 Control

When it comes to control, the balance between the increase in power absorption and the complexity of the system has to be found. An control easy to implement in most generators is a variable generator damping, scheduled according to the sea state. However, to maximize the power absorption, the WEC's natural frequency has to match the frequency of the wave. Some systems uses

specialized mechanisms to change the natural frequency of the WEC [21], while other just change the generator damping and consequently the damped frequency of the WEC. Quite often the latching or declutching approach proposed by Budal and Falnes [22] is used: Here the translator is latched or freely moving until the desired phase offset between WEC and wave is reached. For all controlled systems, the biggest challenges is to find the best control parameters, as the waves are changing constantly.

Conventional approaches
Optimal control as investigated in [23, 15, 16] requires a very accurate mathematical model of the system, especially constrains are hard to implement [24]. Model-predictive control as in [25], uses a model of the WEC to find the best scenario for a specific time horizon. Also here the quality of the control is related to that of the model. Many model based approaches rely therefore on a good characterisation of the system, which may be difficult to obtain in the real world.

Machine learning approaches
In recent years, control using machine learning have become popular. Here the control strategy is not implemented manually, instead it is trained autonomous on a set of data. Notable approaches in the field of wave energy can be found in [26, 27].

1.3 Research question

This thesis is addressing the challenges in controlling a WEC by looking for a robust and model-free control strategy that increases the power absorption of floating point wave energy converter in an array.

Also this thesis focuses on strategies suitable for different types of wave energy converter (and even energy converter in general), for the numerical simulations and physical experiments a specific device had to be chosen. Therefore a floating point wave energy converter inspired by the WEC designed at Uppsala University was selected: A floating point absorber with bottom mounted direct driven linear generator. This design is very simple, allowing to get more universal results. Furthermore many similar concepts can be found, making it easier to compare the results to other devices.

1.4 Outline

In order to approach the thesis's aim, several steps had to be undertaken: Physical scale model were designed for wave tank tests and a numerical model was development to validate the control strategies. The influence of the PTO

inertia and damping on the power absorption were evaluated and possible optimized layouts and their influence on the control were discussed. On base of these findings the collaborative learning control approach aiming to increase the power absorption of WECs in an array was developed:

- An uncontrolled approach with using a high inertia PTO to match the wave frequency is tested as the contrary approach to a controlled WEC (Paper I).
- The characteristics of the Wave Energy Converter were investigated while performing a power matrix with optimal damping control for a single WEC. This was done in simulation and for the physical scale model (Paper II).
- Wave farm optimization can not be done by focusing on the control only, the layout also needs to be considered. The layout of the array may influence the optimal control parameters, while it also determine what kind of control strategies may be used. Therefore investigation is also undertaken on how a optimal WEC farm layouts may look (Paper III).
- Finally, the Collaborative Learning (CL) is presented, which makes use of the array configuration for a robust and model-free control strategy. Here, several WECs in a row apply different strategies. The result of each strategy helps to train a machine learning algorithm, who will then be able to find suitable parameters for a specific sea state. This strategy is used for generator damping (Paper IV) and latching control (Paper V).

The next chapter will focus on the theory that is used in this paper, followed by the presentation of the collaborative learning algorithm in chapter 3. Chapter 4 presents the results of the numerical simulation and the wave tank tests, before chapter 5 discusses these results. The last chapters will give a conclusion of this thesis and a outlook on future work.

It took hundreds of years and a lot of invention, but then a tradition from Hawaii spread out into the whole world and become modern surfing. This thesis wants to contribute that the same will happen to wave energy one time.

2. Theory

This chapter will explain briefly the theoretical background for the methods used. It starts with the theoretical background of the linear potential wave theory which is used for the numerical simulation presented in the next chapter, before continuing with a short description about the fundamentals of wave energy absorption with heave buoy type converters. Common control strategies are presents and from this the ones investigated in this thesis are chosen. A special focus is put on machine learning which was used for a novel collaborative control. The basis, artificial neuronal networks are introduced in the last section of this chapter.

2.1 Numerical wave modelling

2.1.1 Linear wave theory

While interacting with the ground, objects in the water and themselves, the dynamics of water waves are very complex. With the increase in computational performance, it became possible to use simulate thousands of water particles at the same time, leading to very accurate results. These methods are known under the name Computational Fluid Dynamic (CFD) and are used for a wide field of application. Unfortunately they are very resource consuming. In the field of marine and naval engineering, where multi-body wave interaction and large areas have to be simulated, a simplified but - while staying inside the limitations as listed below - still accurate simplification is used: The linear wave theory.

The basic assumption of linear wave theory is that the fluid is inviscid, incompressible and irrotational and the waves are non-steep [28], small compared to the water depth, the body motion is small and gravity is the only force acting on the fluid, what is in good agreement given for the waves under consideration in this study.

Having an incompressible fluid the fluid velocity in all dimension has to equal out:

$$\nabla \vec{v} = \frac{\partial u}{\partial x} + \frac{\partial v}{\partial y} + \frac{\partial w}{\partial z} = 0 \tag{2.1}$$

where $\vec{v} = (u\, v\, w)$ is the fluid velocity in all directions. The irrotational fluid allows to introduce the velocity potential Φ, a scalar that is defined as the

negative of the partial integration of u, v, w, along x,y and z. With that 2.1 becomes:

$$\nabla\vec{v} = \frac{\partial^2\Phi}{\partial^2 x} + \frac{\partial^2\Phi}{\partial^2 y} + \frac{\partial^2\Phi}{\partial^2 z} = 0 \tag{2.2}$$

which is well known as the Laplace equation.

Next, the boundary conditions have to determined: First it is assumed that there is no vertical water movement at the sea bed:

$$w(x, z = -h, t) = \left.\frac{\partial\Phi}{\partial z}\right|_{z=-h} = 0 \tag{2.3}$$

The surface condition (z=0) is split into kinematic and dynamic conditions. At the free surface the velocity potential in z-direction is determined by the surface elevation $\eta(x,t)$ (kinematic surface condition):

$$\eta = -\frac{1}{g}\left.\frac{\delta\Phi}{\delta t}\right|_{z=0} \tag{2.4}$$

and at the same time the pressure at the surface must be constan (dynamic surface condition):

$$\left[\frac{\delta^2\Phi}{\delta^2 t} = -g\left.\frac{\delta\Phi}{\delta z}\right|_{z=0} \tag{2.5}$$

Based on these conditions the wave field can be calculated and so, via integration over the wetted surface all hydrodynamic parameter.

2.1.2 Wave Body interactions

A wave interacts with a body in three ways:

- The incident wave ϕ_i causes a pressure on the object's wetted surface A_w and so a force. If the object is not fixed, it will start to move and so
- radiate a wave ϕ_r, which will spread out and so influence the incident waves of bodies nearby.
- Each body in the water is a obstacle for the wave, causing the wave to scatter ϕ_d.

When the hydrodynamic coefficients are known the forces on the object can be calculated. The excitation force is calculated by integrating the velocity potential over the wetted surface A_w:

$$F_{e,j} = i\omega\rho \iint_S (\phi_0 + \phi_S) n_j dS\,, \tag{2.6}$$

with n_j being the normal vector in direction j [29, 28]. The excitation force may cause a movement of the body. While focusing on heave (direction: z) point absorbers, only motion in heave direction is considered; surge and sway are seen as neglectable which is in good agreement with experimental tests [30].

2.2 Control of Wave Energy converters

2.2.1 Wave energy absorption with heave buoy type converters

For simplification a one degree of freedom (heave direction) single body (buoy and generator have a fixed connection) floating point absorber with a fixed generator damping is considered in this section. In calm water, the system can be seen as an harmonic oscillator with a damped frequency of:

$$\omega_d = \sqrt{k/M_t - 0.5d/M_t}, \tag{2.7}$$

where d is the overall damping (the sum of the generator damping γ and the hydrodynamical damping), k is the buoyancy stiffness and M_t the total mass of inertia. As d is fixed, the absorbed power $P_a = \gamma v$ depends only on the velocity v, and so the absorbed energy for a forced oscillation with frequency ω is:

$$E \sim \hat{F}/(j\omega M_t + d - jk/\omega), \tag{2.8}$$

with E being the absorbed energy and $\hat{F}$ the amplitude of the force. From 2.8 follows that the energy absorption is maximized when

$$M_t = k/\omega^2. \tag{2.9}$$

If condition 2.9 is fulfilled, the WEC has the same natural frequency as the forced oscillation (e.g. sea state).

If the WEC is in resonance and the damping is matching the sea state, the theoretical maximum is reached. However, the influence of the natural period is much higher than the influence of the damping.

From this four important conclusion can be drawn:

- The generator damping γ can be used to adjust the damped frequency and so increase the power absorption
- The power absorption for a fixed damping is maximized if the natural frequency matches the wave frequency. The natural frequency of the WEC can be changed by either altering the spring constant of the system or the inertia.
- The maximal power is absorbed if the WEC is in resonance, and the damping matches the sea state.
- The influence of the natural frequency on the power absorption is much higher than the influence of the damping.

2.2.2 Challenges with energy absorption of WECs

In reality, one body WECs can be rarely found. The WECs considered in this thesis for example have two bodies (buoy and generator) which are connected via a line. If the line is slack the characteristics of the system differs from the characteristic when the line is tensioned.

Furthermore the interaction between the WEC and the wave has to be considered: The radiated wave is related to the speed of the buoy: On one side

a measure of the absorbed power by the buoy, on the other side, due to the interaction with the incoming wave, it also reduces the power that can be absorbed. In arrays the influence of the radiated wave on neighbouring WECs have to be considered.

Finding the optimal frequency for a WEC can be challenging for ocean waves, as they are in general irregular waves, superposition of waves with different frequencies. If such a sea spectra is constant for a time interval, it is called a sea state. The distribution of sea states at a specific location is known at the wave climate. So there is not one single optimal frequency, in fact the optimal frequency is changing over time, and is in general not known in advanced.

2.2.3 Control strategies

Over the time different control strategies for WECs have been developed, focusing on different aspects: Beside the absorbed power, the parameters that are controlled, the need of a theoretical model and the robustness are important aspects of a control strategy. This section will give a brief overview over state of the art control strategies, a more detailed discussion can be found in [31].

Controllable values

A comparable easy to implement option is to change the damping of the generator. In case of an electric generator, this can be done by altering the load. Some systems may furthermore allow to tune the natural frequency of the WEC with adjustable stiffness of additional inertia. But more convenient are systems that change the oscillation frequency of the WEC by manipulating the motion of the power take, for example by decoupling the translator from the buoy motion, or by stopping the motion of the PTO [22].

No control

Some WECs, like the UU-WEC, use no control to simplify the mechanics. Depending on the design, the WEC will capture significantly less power than the theoretical optimum, but for a wide range of sea states. Or it will be tuned for a specific sea state where it reaches the optimum, but will show a poor capture performance outside these sea states.

Complex-conjugate control

A controllable spring stiffness or inertia, together with an adjustable damping enables a control strategy that fullfills condition 2.9 with optimal damping for every wave. Complex-conjugate control will lead to the highest power absorption, but systems with tunable inertia or spring stiffness require complex mechanism and are rarely found. An example for such devices can be found in [21].

Figure 2.1. Latching sequence of the second buoy: In the first picture the buoy is latched and noticeable lower than the other buoys. Between picture 2 and 3 the buoy is released and 'jumps' up. In picture 6 the buoy is latched again (From Paper V).

Latching and declutching
For WECs with fixed oscillation frequencies higher than typical wave periods, the latching control was proposed. Here, a phase offset between wave and WEC is created by latching the WEC and releasing it after a latching time t_l. This time depends on the difference between wave period and oscillation period of the WEC. The opposite control strategy for WECs with a lower oscillation frequency is called declutching, here, the PTO is detached. An example of a latching buoy can be seen in Figure 2.1.

Control parameter estimation
The problem of all presented controls is the determination of the best parameters. In the following three methods used to find the best control parameters are described:

Optimal control
Assuming the control problem is accurately described with differential equations, the search for optimal control parameter can be done with ordinary optimization methods (Hamilton-Jacobi-Bellman). The first step is to introduce a cost function stating the weighting of different factors that have to be considered in the optimization. The next step is to solve the equation. However, it is not always possible to get a suitable mathematical model of the control problem: Non-linearities like constraints are difficult to implement and very often a detailed parametrisation of a WEC is too complex.

Model-Predictive Control
To achieve the optimal power absorption a controller has to look forward. The idea of model predictive control (MPC) is, to provide the controller with a model, which can be used to simulate the impact of the current action on the further power absorption, and so look for the scenario which increases the power absorption. The prediction is updated at each time step to consider possible differences between prediction and reality. MPC is successfully used in many areas. An example for a MPC for wave energy converters can be found in [25]. The quality (or more precisely: the prediction horizon) of an MPC relies strongly on the accuracy of the model. Especially the complex interactions of WECs in general, and for WEC arrays in particular may increase the complexity to develop a suitable controller for realistic conditions.

Machine learning

In recent years machine learning algorithm have been used to solve many problems which are otherwise hard to describe. No model of the process to be controlled is needed. Due to the complex interactions between buoy and wave and the constraint and non-linearities of the PTO, machine learning was tried earlier successfully in wave power applications [33, 34]. In this thesis two machine learning approaches are used: Genetic algorithm were used to optimize the array layout in Paper III and artificial neural networks (ANN) were used in the collaborative learning algorithm in Paper IV and V.

2.2.4 Control strategies used in this thesis

The aim of this thesis is to find a control for wave energy converters in a farm which will work under realistic condition. Therefore the robustness is seen as an important aspect. As obtaining a good and reliable model and parametrization is still a challenge for WECs, a model free control was chosen, excluding optimal and model predicting controllers.

The easiest way to operate a WEC is using no control. This was tested in Paper I with a special WEC with an optimized natural frequency. The next step was to test the performance of an optimized generator damping in Paper II, a control value that is comparably easy to implement. The main focus of this thesis lies on the collaborative learning, which is a control strategy based on machine learning and was implemented with latching (in Paper V) and damping (in Paper IV) control. As learnable element artificial neural networks are used, which are explained in the next section.

2.3 Artificial Neuronal Networks

Within the area of machine learning, artificial neuronal networks (ANN) stick out due to their good performance in application where analytical methods are hard to implements, such as speech recognition [35], picture recognition [36], artificial intelligence [37] and wave prediction [38]. ANNs are so-called black-box models, meaning that no information about the task to perform is necessary. In the beginning the ANN is just structure, that adapts to its specific task by learning. Learning can be done in three fundamental ways:

- Supervised learning means that a data set linking input and desired output data is used to train the ANN, which tries to change its structure so that it finds a function describing these linkage.
- Unsupervised learning on the other side does not need a data set with referenced values. The network gets data and tries itself to classify them into categories. An example for such networks are self organizing maps.

- Reinforcement learning does like unsupervised learning not need any reference value, instead it needs an evaluation function that is judging over its output. The ANN will take some action on basis of the input, the results of the action are then judged and a positive or negative reward is feed back to the network; the aim of the ANN is to find the output values for an input value that lead to an positive reward.

Supervised learning is maybe the most popular of these learning strategies, as it is the most direct and fastest one. However, a large data set of labelled data is needed. This is not required for reinforcement learning, which is in return not as effective as supervised learning and depends heavily on how accurate and quick a specific output can be rewarded.

Networks types

The name artificial neural networks comes from the fact that they were inspired by the brain structures in animals. However, despite some similarities artificial neuronal networks used for machine learning are much simpler than biological ones. While in biological neuronal networks connection between neurons are unordered and contain many feedback loops, they are often more ordered and feedback loops are limited in artificial ones. In the following three common network types are presented:

- The widely used multi layer feed forward perceptron networks classifies the neurons in layers. Each neuron of a layer feeds its signal forward to all neurons in the next layer. However, backward connections or connections skipping one layer are not allowed. The output is only dependent on the current input, temporal dynamics are not considered.
- Recurrent networks allow backward connection, and so allow to have internal states. But due to stability reasons they are mostly used in the form of short-long term networks which limits the feedback [39].
- Convolutional layers can be used with both network topologies. Convolutional layers played an important role for many recent advances in artificial intelligence [37, 40] and picture recognition [36]. Theoretically a non-convectional network can act the same, but only for the cost of much more layers.

Paradigmas

Beside the network types, two paradigms are common with neuronal networks. The traditional paradigm is to use small networks with just a few neuron layers, but pre-processing the input data easing the learning process for the network. While the computer performance increased significantly in the last years, the paradigm of the "deep" network, using more layers while reducing the pre-processing of the input data evolved. Especially in combination with convolution networks these networks established new records in the field of artificial intelligence, non-linear control and speech and image processing.

Working principle

The basic working principle of a neuronal WEC is now explained with an artificial neural multi layer feed-forward perceptron network The smallest part of an artificial neural network is the neuron, also called perceptron or unit. In each layer l a number of n_l neurons are placed. The first layer receiving the input values is called input layer, the last layer is analogues called output layer; all layers in-between are called hidden layers. A neuron j in a hidden or output layer l has exactly one input connection to each neuron in the previous layer. It takes each input times a weight $w_{i,j}$ where i is the neuron the signal comes from. This leads to a $n_{l-1} \times n_l$ weighting matrix W for layer l. To the weighted input a bias b_i is added, the result is called potential p_i. This potential is input of a non-linear activation function f_A, which determines the output of the neuron. Common activation functions are the logistic function for networks with a few layers and the ramp function (neurons using this function are often called rectified linear units, ReLUs). In the input layer neurons have no input weights and only one input: the input data. The number of neurons in the input layer is equivalent with the number of input scalars. Similar the number of neurons determines the number of output scalars. When the output neurons represent probabilities of a classification or action, the softmax function may be used to determine the neuron with the highest probability.

Learning

Learning is done by adjusting the weight regarding the influence of the weight on the output error e, expressed with δ:

$$\delta_j = \frac{\partial e}{\partial w_{ji}} \tag{2.10}$$

The error is first calculated fo each output neuron by comparing the output $\vec{o}$ of the network to reference data $\vec{r}$ to calculate the square error $\vec{e}$ for each neuron:

$$e_i = 0.5(r_i - o_i)^2. \tag{2.11}$$

And so δ becomes:

$$\delta_i = (r_i - o_i) \tag{2.12}$$

For the hidden and input layers, the error has to be back propagated, so δ is calculated:

$$\delta_i = \sum_{j=0}^{n-l} (w_{ji}\delta_j) \frac{df_{A,j}(p_j)}{do_j}. \tag{2.13}$$

The weight is than updated with a specific learning rate η:

$$w_{ij} = \eta \delta_j o_i. \tag{2.14}$$

A too high learning rate will increase the chance that a minima is missed and may lead to an unstable system, a lower learning rate will reduce these risk, but will also slow down the learning.

2.4 Array layout

As WECs in an array interact with each other, optimal control and farm layout depend on each other. In order to know how a optimized layout for WECs may look like, this was investigated in Paper III: For three different scenarios (see Table 2.1) the optimal configuration was searched with a genetic algorithm (GA).

Table 2.1. *Overview of the scenarios (scen.) used in the layout optimization; The layout grid spacing is 15 m in each direction.*

scen.	WECs	Layout	Optimization value	parameters
1	9	3x3	non-dimensional power/mass	buoy radius (2 m or 3.5 m)
2	6 large, 6 small	-	total power	layout, 6x6 grid
3	4	2x2	power/mass	buoy radius: $R \in [2 : 0.5 : 3.5]$ m, buoy draft: $d \in [0.3 : 0.05 : 0.6]$ m, PTO damping: $\gamma \in [15 : 1 : 250]\ \frac{kNs}{m}$

2.4.1 Experiments

Genetic Algorithm

Genetic algorithms are biological inspired optimization strategies. The set of variables is seen as a chromosome, where each variable is a gen. Several chromosomes, so possible solutions for this optimization problem, form a population. All chromosomes in a population are evaluated and rated on base of a cost (or in GA terminology fitness) function. Only from the best rated chromosomes the gens are mixed (normally in pairs of two) and slightly changed (mutation), so that a new set of possible solutions (new generation) is created. More details can be found in Paper III.

Cost function

Three cost functions are used. For the first scenario the non-dimensionalized power absorption to mass ratio is used:

$$f_{C1} = -\frac{(P_t - P_s)/(P_b - Ps)}{(m_t - m_s)/(m_b - ms)}, \tag{2.15}$$

where P_t is the total absorbed power, P_s the absorbed power when all buoy have the smallest radius and P_b the absorbed power when all buoys have the biggest radius. The second case uses the absorbed power as cost function and case three the ratio between total absorbed power and total mass.

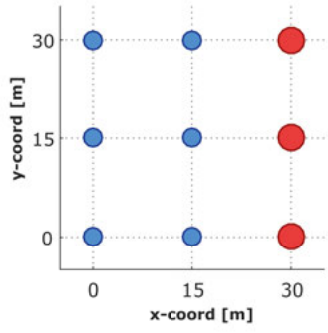

Figure 2.2. Best solutions of the GA for case 1 (From Paper III).

WEC sizes
A WEC inspired by the UU-WEC was used to perform the tests. In case 3 the parameters of the WECs were chosen by the GA, in case one and two the two different WEC sizes were used:

- The small WEC has a radius of 2 m and a mass of 6440 kg, resulting in a draft of 0.5 m. The generator damping is 70 kNs/m.
- The large WEC has a radius of 3.5 m and a mass of 23668 kg, resulting in a draft of 0.6 m. The generator damping is 200 kNs/m.

Evaluation
The solutions were evaluated with a linear frequency domain model of the wave park.

2.4.2 Optimal Array

The result for case one can be seen in Figure 2.2. Two rows with three small WECs and one row with three large WECs are placed parallel to the wave front. The solution for case 2 can be seen in Figure 2.3. Both solutions, the best and the worst, look a bit chaotic. This might be an indicator that the GA has not found the optimal solution yet. A qualitative guess how the optimal layout could look like can be seen in Figure 2.4. The best solution of the GA optimization of the WEC parameters can be seen in Figure 2.5. The four WEC differ only slightly in the generator damping (which is about 2.7% higher in the second row seen from the wave direction), but are otherwise equal.

2.4.3 Discussion under the aspect of control

It is remarkable in Figure 2.2 and 2.4 that the WECs in a line parallel to the wave front are the same. Also when looking on the original solution of the second case in Figure 2.3, it can be seen that in the worst case the WECs are

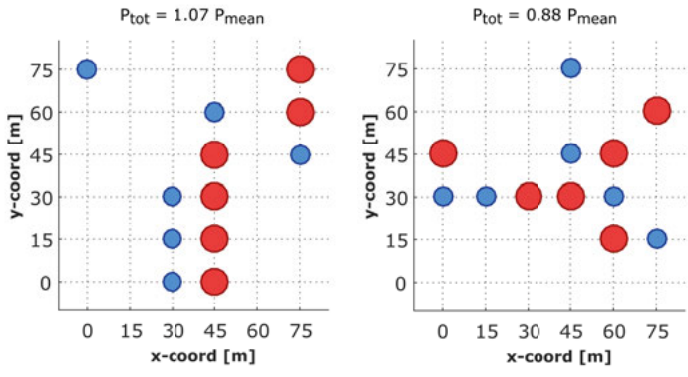

Figure 2.3. Solution of the GA for case 2. The best solution is on the left, the worst on the right (From Paper III).

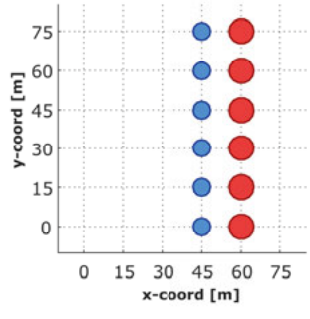

Figure 2.4. Guess how the ideal solution for case 2 could look like (From Paper III).

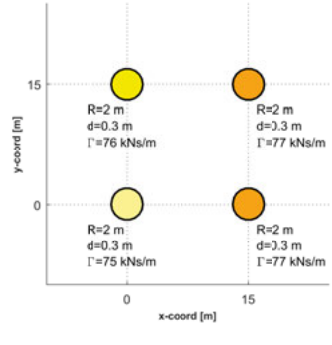

Figure 2.5. The best solution of the GA for case 3 (From Paper III).

located unordered in the whole grid, while the best solution is dominated by equally sized WECs ordered in lines parallel to the wave front. According to this results, a WEC controller can focus on grids with rows of identical WECs. Moreover, from Figure 2.5 it can be argued, that the WECs in an array may have similar parametrisation and the optimal generator damping (which is often the only control parameter) is almost independent of the position.

3. Methods

The control strategies presented were tested in both numerical simulation and wave tank tests. First, the numerical simulation used in Paper I, II and V is described which is based on linear potential theory and is able to simulate single WECs as well as WEC arrays and allows to control each WEC with a range of control strategies. Then the simplification made on the numerical simulation for Paper IV is introduced.

All control concepts were also tested in 1:10 scale physical experiments in the wave tank of the COAST laboratory at the University of Plymouth. Two experimental models were used: The active model allows to simulate all kind of controls, while the passive one can only perform constant damping. Both are introduced in section 3.3.

The last section of this chapter deals with the collaborative learning, the model free machine learning based control strategy which was developed for WECs in an array.

3.1 Numerical Simulation

The hydrodynamic parameter were calculated by WAMIT, a hydrodynamic solver based on the linear potential wave theory described in the last chapter. The outputs, impulse response functions (indicated with f, while forces are indicated with F) of the excitation wave force (including the incident wave force and the scattered wave force $F_{e,j}(t) = F_{i,j}(t) + F_{s,j}(t)$) and the radiated wave $F_{r,j}(t)$ for all WECs in the array where then used in the numerical simulation. The buoy and PTO were the same for all WECs involved in each array. The simulation models the WEC as a two body system (buoy and generator) and the connection line as a damped spring. A similar models was validated for full size WEC data in [41].

Buoy
For the buoy j (position x) the equation of motion is:

$$\ddot{x}_j = (F_{e,j} + F_{r,j} + F_{h,j} + F_{l,j} + m_b g)/(m_b + m_a), \tag{3.1}$$

where F_l is the line force, m_b is the mass and m_a the added mass of the buoy. The other forces are: The excitation force F_e is the force on the body caused by the incident wave and decreased by the scattered wave:

$$F_{e,j}(t) = (f_{e,j}(t)) * \eta(t), \tag{3.2}$$

where $\eta(t)$ is the wave elevation. The hydrostatic force F_h is the product of the buoyancy at equilibrium draft and the position of the buoy below the surface (x):

$$F_{h,j}(t) = b_b x_j(t). \tag{3.3}$$

The buoyancy is calculated as the product of the cross-sectional area of the buoy on the water surface A_w, the water density ρ and the gravity acceleration g. The force on WEC j caused by the radiated waves of all n buoys is:

$$F_{r,j}(t) = \sum_{k=0}^{n} f_{r,j}(t) * \dot{x}_j(t). \tag{3.4}$$

Line
The connecting line force $F_{l,j}$ is non-linear, depending if the line is slack or tensioned:

$$F_{l,j} = \begin{cases} c_l(x_j(t) - y_j(t)) + d_l(\dot{x}_j(t) - \dot{y}_j(t)) & , x_j > y_j \\ 0 & , \text{else} \end{cases}, \tag{3.5}$$

with y being the position of the translator, c_l being the line elasticity and d_l the line damping.

Generator
The characteristics of different generators may vary significantly. Therefore the generator is not part of the main software, but different profiles can be loaded via library files. Unless otherwise stated in the experiment description, an idealized velocity dependent generator force with the damping factor γ is used. With m_w being the translator weight, the equation of motion for the generator is:

$$\ddot{y} = (\gamma \dot{y}_j(t) - F_{l,j} + m_w g)/m_w. \tag{3.6}$$

A modification of the ideal linear generator can read the control libraries as used by the physical set-up (see later in this chapter), so that the same control strategies can be used in physical and numerical experiments.

The coupled equation (3.1), (3.5) and (3.6) were solved using a delayed differential equation solver (DDE) with a fixed step-width of 1 ms. The inputs are the wave time series, the number of WECs to be simulated, the parameters for the buoy, the line and the PTO and the generator model that should be used for each WEC (including a possible control strategy). The output is the position and velocity of both translator/rotor of the generator and buoy as well as the absorbed power. Figure 3.1 gives an overview of the simulation. This model was used in Paper I, V and II.

3.2 Simplified Numerical Simulation

For the CL latching control in Paper IV a simplified version of the model is used to speed up the learning process. While translator and line modelling

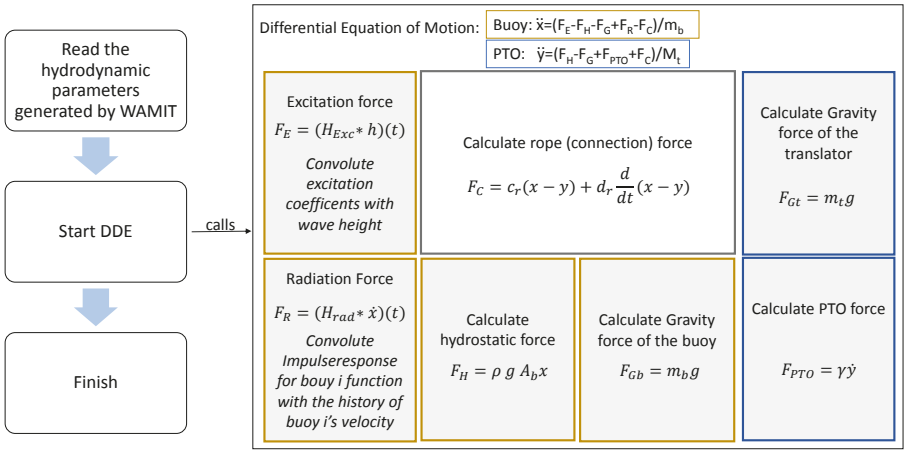

Figure 3.1. A block diagram of the numerical simulation including all revelant equations (From Paper II).

is analogue to the model described above, the hydrodynamic interactions are simplified: It is also assumed that the WECs in the array have no interactions among each other; the scattered wave is neglected and effects of radiated waves are expressed in a linear buoy damping constant b_d. The so obtained model is not relying on the impulse response function what makes it causal. The added mass and the buoy damping constant where determined from a decay test of the buoy. A sketch of this model is found in Figure 3.2.

Heave force

According to Bernoulli's principle the force can be described as a potential force F_{Bc} and a kinematic force F_H, both are depending on the surface elevation h, the buoy's position x and the projected wetted surface of the buoy A_B. The potential force $F_{Bc} = \rho g A_B(h-x)$ is called buoyancy stiffness. The kinematic force is

$$F_H = \begin{cases} A_B\rho(\dot{h}-\dot{x})^2 & , x < h \wedge \dot{h}-\dot{x} > 0 \\ 0 & ,\text{else} \end{cases} , \tag{3.7}$$

where ρ is the density of water (here set to 1000 kg/m^3).

Buoy

The buoy is modelled as a linear spring-mass-damper system, with the equation of motion:

$$\ddot{x} = \frac{F_H + F_{Bc} + F_{Bg} + F_r + F_{bd}}{m_B + m_A}, \tag{3.8}$$

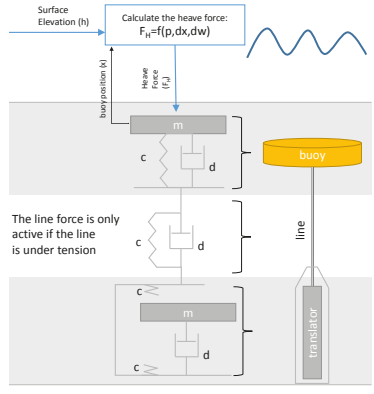

Figure 3.2. A sketch of the simplified numerical simulation; c indicates a spring stiffness, d stands for a damping factor, and m symbolises a mass..

with F_L being the line force, $F_{bd} = d_b\dot{x}$ being the linear damping of the buoy, m_B being the mass and m_A being the added mass of the buoy and $F_{Bg} = M_b g$ being the gravity force.

3.3 Physical modelling

Two physical models were used. The active model (in use in Paper II, IV and V) uses an electric motor as power take off which can mimic a wide range of control algorithm, while the passive model (used in Paper I) is able to accurately simulate PTOs with an ideal constant damping and was used to study the influence of the inertia of the PTO on the absorbed power.

During the wave tank tests, both systems are located on a gantry over the wave basin. The line attached to the PTO is guided by a pulley system over the top of the gantry to the bottom of the wave tank (see also Figure 3.3), from where it is distributed to the corresponding buoy. This systems offers the possibility to accurately simulate a seabed based generator without the need of having a waterproofed PTO. It furthermore gives a great flexibility in the positioning of the buoys.

3.3.1 Active PTO

The active PTO consists of a tubular electric motor of type Parker ETT-080 for single buoy experiments or ETT-050 for up to four buoys simultaneously, both provide a stroke length of 330 mm. Springs on the ends of the casing prohibit damage to the structure in case the translator exceeds the stroke length. A force sensor of type Megatron KT1101 is mounted between translator and line, see also the photo of the set up in Figure 3.3.

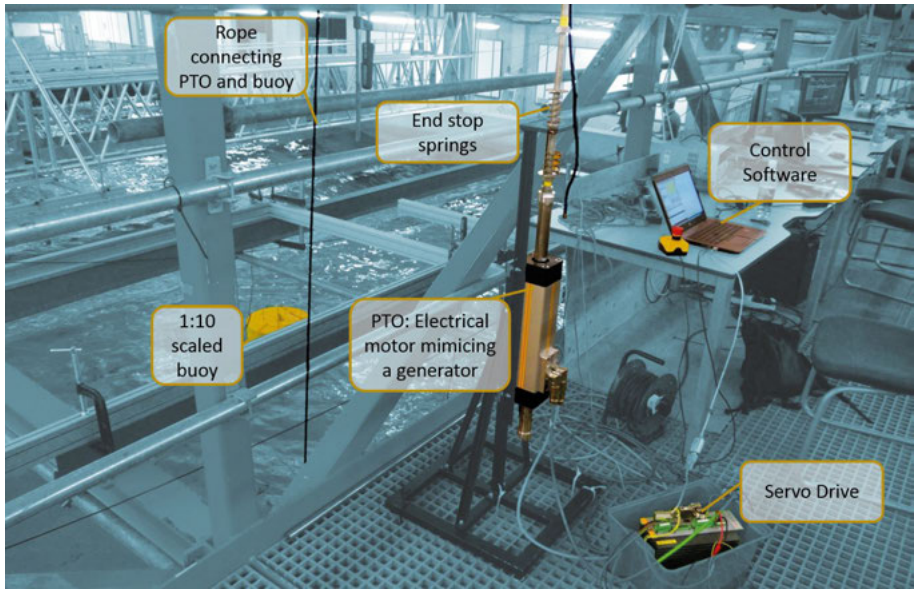

Figure 3.3. Set up of the active PTO for the single buoy experiments in Paper II. Also the motor model was changed for other tests, the overall set-up stayed the same for all tests.

Control system

The control of the motor is done in three cascades. Cascade one is the servodrive of type Parker Compax 3 which allows to control the motor in the following ways:

- The current control mode allows to specify a specific current to the motor which will induce a force.
- The velocity control mode allows to specify a the velocity of the translator, which the servo drives tries to achieve.

The servodrive itself is connected via Profibus to the control computer, that sends the reference data, so that the motor mimics a generator (Cascade 2). The third cascade is the library with the specific control strategy, which is also running on the control computer. The programming interface is the same as for the numerical simulation (see above), so that the same implementations can be tested in the numerical simulation and in the wave tank test. Cascade 1 is executed with 8 kHz, while Cascade 2 and 3 run with 100 Hz.

To achieve a reliable constant damping, two different concepts for the controller in the second cascade were tested:

- In Paper II the current control mode was fed with an electric current proportional to the velocity, in order to simulate the generator damping. Due to dead times and noise, the system was instable; first a filtering of the velocity input, leading to an approximately 25 % smaller damping force could resolve this problem. This strategy was

enhanced for the tests in Paper V were a proportional-derivative filter was used to compensate the integral characteristics of the system and improve the dynamics. However the dead times couldn't be reduced.

- In Paper IV the velocity control mode is used. The input force is measured by the force sensor and then a model calculates the corresponding acceleration and so the actual speed. This algorithm had problems while taking the inertia of the translator into account, as it leads together with the limited dynamic of the translator to small oscillations also in calm water.

3.3.2 Passive PTO

The damping of the passive PTO is achieved by using an eddy current break: An aluminium disc is rotating within the magnetic field created by magnets mounted on a vice. Only the movable jaw is equipped with magnets, the fixed jaw may work as back iron if the gap is small enough. By changing the jaw gap, the distance between the magnets and the disc can be varied and so the induced eddy current in the disc which provides the system with a nearly ideal linear damping. A winch is fixed with the aluminium disc, on which a line is leading towards the buoy and another line is fixed with the weight. The induced forces will cancel each other in calm sea state. Compared to a traditional linear generator WEC, the aluminium disc will lead to a high inertia of the system. The specific set-up was build using a bicycle wheel truing stand (Tacx T3175) with a hub for disc breaks mounted (Shimano XT HB-M756), but instead of the disc break the aluminium disc is mounted. The alloy AL1050 was chosen, as it is a good compromise between weight and electric conductivity. The disc has a diameter of 40 mm and a thickness of 2 mm. On the disc a inertia measurement unit (IMU) acts as an absolute encoder of the disc's position and the velocity, see Figure 3.4 for details about the data processing The magnets on the vice are five Neodymium N42 squares with a size of $20x20x10$ mm. A sketch can be found in Figure 3.5.

3.4 The collaborative learning algorithm

While working with WECs in an array the search for optimal controlling parameters can be parallelised. This solves a big problem: In reinforcement learning the actions of the agent (here a WEC) have to be judged with a positive and negative reward. With collaborative learning several parameters are tested simultaneously, so that the most beneficial of these parameter can be easily determined, and so reference data for the machine learning is obtained.

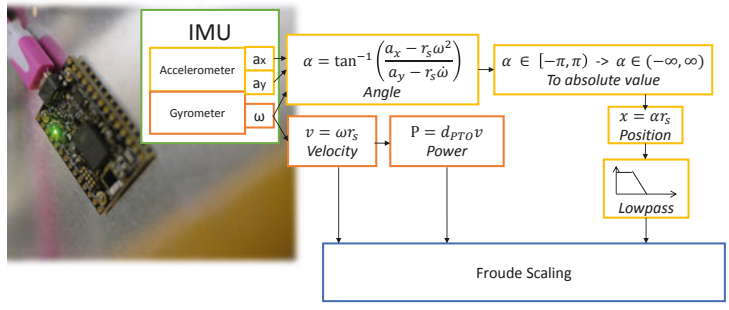

Figure 3.4. Data processing from the measurements of the IMU till position and velocity data (from Paper I).

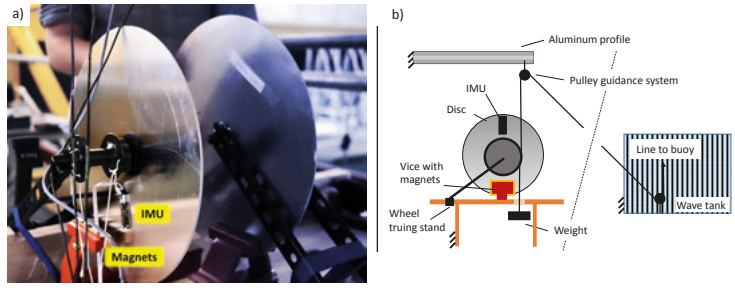

Figure 3.5. Sketch of the passive PTO (from Paper I).

3.4.1 The CL process

Several WECs, all applying different control parameter, but are otherwise identical are placed parallel to the unidirectional, irregular wave crest. At least one of the WECs has to be learnable.

1. The central WEC sends a start signal.
2. All WECs apply their control strategy according to their internal policy based on the actual sea state.
3. The central WEC sends the stop signal.
4. All WECs report their absorbed power and their applied control parameters to the central WEC.
5. The central WEC selects the control parameter which leads to the highest power absorption and feeds it back to the learnable WECs.
6. The learnable WECs adapt their policies.
7. The process starts again at 1.

The CL algorithm was implemented to control the generator damping in Paper IV and to choose the best latching time in irregular sea states in Paper V. In both implementations constant WECs (cWEC) and learnable WECs (lWEC) were used. A cWEC applies always the same damping factor or latching time, while a lWEC is equipped with a machine learning algorithm and selects the control value based on its policy.

For the damping control, the WECs recorded the line force, the applied damping and the absorbed power (all together called a sample) with a sampling frequency of 1.15 Hz. The duration between 'start' and 'stop' signal was fixed with 3 s in the simulation and 6 s as full scale equivalent in the wave tank tests. The input data for the machine learning algorithm was a series of the latest four reading of the force sensor data for each sample. The output was the damping coefficient.

Due to the non-linear movement during latching, the information about the sea state could differ between the WECs. Therefore a central WEC without latching is introduced for CL latching: It measures the wave to synchronize all WECs. When it detects the first crest or through it raises a start (or latch event) and sends the mean wave period of the last seven waves to all WECs. All WECs choose their latching time based on the information about the mean wave period and according to their policy. The next time the central WEC detects a extrema it sends a stop event and immediately after learning is finished the next start event it raised. The WECs record only one sample, consisting of the applied latching and the absorbed power for each latch event. The input data for the machine learning algorithm is the mean wave period, the output is the latching time.

3.4.2 Design of the ANN

For both control strategies ANNs are used for machine learning.

CL Damping

In Paper IV the damping control uses a time series as input. A 'deep' network approach with eight hidden layers and a 'shallow' approach with just 2 hidden layers were chosen. The 'shallow' network is furthermore equipped with a exploration algorithm. In both cases, the output was a single neuron representing the damping factor.

CL Latching

For the latching control in Paper V a very basic ANN is used, consisting of just nine hidden neurons distributed over three hidden layers. The mean wave period is fed into the input layer consisting of 10 neurons, each representing a specific time interval. The output layer is made of 13 neurons of which each is assigned with a latching period. A SoftMax function calculates the probability for each latching time.

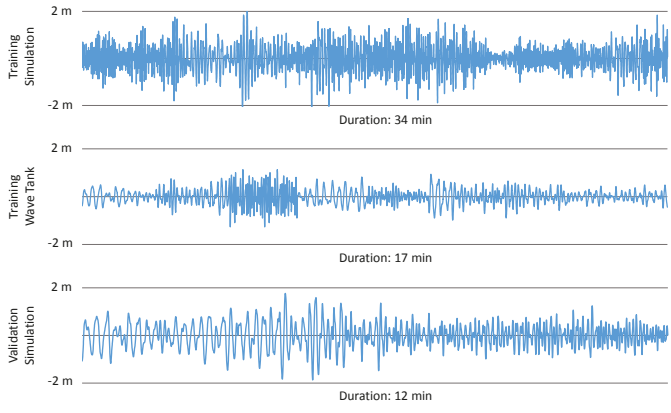

Figure 3.6. The evaluation and training waves (from Paper V).

3.4.3 Mean wave period correlated latching time

As reference for the latching strategy a latching time linearly related to the mean wave period was chosen:

$$T_L = c\,\overline{p}_w\,, \tag{3.9}$$

where c is the linear correlation coefficient, T_L the latching time and $\overline{p}_w$ the mean wave period. Assuming a regular wave with a period much lower compared to the oscillation period of the WEC, then the optimal latching time is $1/4$th of the wave length, so that the phase offset between wave and translator motion is 45°. An evaluation in the training sequence (see below) with the numerical simulation resulted in a optimal latching time of 0.22 of the mean wave length for the WECs.

3.4.4 Wave Sequences

To train and test the CL strategies in different sea states, wave sequences containing several Brettschneider spectra sea states were used. Each sea states lasts for approximately half a minute, before the next sea state starts. A overview of all these sequences can be found in figure 3.6. The wave sequences used for learning are longer than these used for evaluation. Two training waves were used: training waves one is made up of sea states up to a significant wave height of 3.75 m, where else the second evaluation sequence uses only sea states with significant wave heights up to 1.75 m. The latter is used for the wave tank test of the CL latching strategy, were high waves were avoided to reduce the forces on the set-up.

4. Experiments

Four methods to increase the power absorption of wave energy converters were tested. Two methods focused on single devices, while the CL strategies are designed for WECs in arrays. The optimized natural frequency WEC (Paper I) was not controllable, in the optimized damping (Paper II) and CL damping (Paper IV) the generator damping was controllable, and in Paper V the latching time was adjusted by the CL. All experiments except the CL latching simulation were performed with buoys of 5 m diameter (0.5 m in the wave tank test). For the numerical CL latching simulation the buoy diameter was reduced to 3.2 m.

WEC design
All WEC designs in the experiments are inspired by the UU-WEC, however, the parametrisation changes slightly between the experiments. Table 4.1 gives an overview over the parametrisation of all WECs simulated during the experiments.

Waves
All tests have in common that the irregular sea states are selected out of a pool of 72 Brettschneider spectra. This spectra is defined as:

$$S(\omega) = \frac{5}{16}\frac{\omega_m^4}{\omega^5}H_s^2 \exp^{-1.25\omega_m^4/\omega^4}, \tag{4.1}$$

where H_S is the significant wave height, the mean wave height of the highest third of the waves. Instead of the modal wave period ω_m, the energy period is used to characterize the spectra:

$$T_e = \frac{\int S(\omega)\omega\, d\omega}{\int S(\omega)\, d\omega}\frac{1}{2\pi}. \tag{4.2}$$

The significant wave heights of the sea states reaches from 0.75 m in steps of 0.5 m up to 3.75 m, while the energy periods are inbetween 3.5 s and 10.5 s, with a step width of 1 s.

4.1 Optimized natural frequency of the PTO

Instead of increasing the power absorption with a control algorithm, here the PTO inertia was optimized, so that the WEC's natural frequency gets close to that of typical sea states.

Table 4.1. *Overview over the WEC parameters in the different experiments in the wave tank (tank) and the numerical simulation (sim.). Ellipsoidal (e) and cylindircal (c) shaped buoys were used. All values are Froude scaled to full scale.*

Test	Optimized frequency		Optimized Damping		CL damping		CL latching	
	tank	sim	tank	sim.	tank	sim.	tank	sim.
Buoy								
shape	e	c	c	c	e	c	e	c
diameter [m]	5							3.2
weight [t]	5		5.3		5			
PTO								
stroke [m]	5	20	3	3	3	3	20	3
transl. weight [t]	5		6		5			
... inertia [t]	46/96	46/120	6		5			
damping [kNs/m]	100	75/125	50-210		200-500		70	
latching	no						yes	

Many floating point absorbers with linear generators, for example the UU-WEC, have a natural frequency lower than the typical wave periods. A heavier translator would lower the natural frequency, but also increase the weight and the dimensions of the PTO.

With the passive PTO the rotating disc brings an extra moment of inertia J into the system: For the translator, the weight resulting in the weight force and the inertia of the translator are always equal, but for the rotating system, the total rotor inertia $M = J/r_l^2 + m_w$ is higher than m_w, allowing to build light-weight systems with a high inertia. The generator equation for the numerical simulation 3.6 becomes:

$$\ddot{y} = (\gamma\dot{y}(t) - F_l + m_w g)/M. \tag{4.3}$$

The inertia m_d of the solid disc is related to the ratio between the disc radius r_c and the radius the line is connected to the disc r_l (and therefore winds up at this radius) (see Figure 4.1 for a sketch of the PTO):

$$m_d = 0.5 m r_c^2/r_l^2, \tag{4.4}$$

the natural frequency can be adjusted just by changing this ratio, while the PTO weight stays the same.

The tests were run with two different PTO inertias (53 t and 101 t).

In the wave tank tests the two inertias were tested in eight sea states with a generator damping of 100 $\frac{kNs}{m}$.

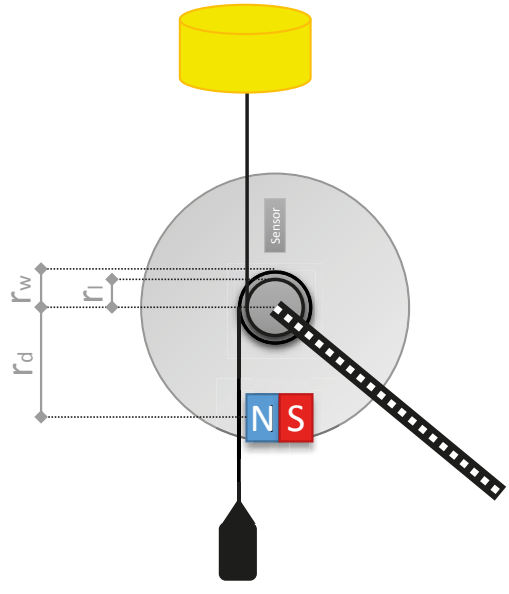

Figure 4.1. Sketch with parameters of the PTO with optimized natural frequency (from Paper I).

In the simulation each of the inertias was furthermore tested with two different generator dampings (75 $\frac{kNs}{m}$ and 125 $\frac{kNs}{m}$) in a power matrix consisting of 17 sea states. To match the results of the numerical simulation and the wave tank experiments, the sea states used in the wave tank test were also simulated using a line with increased elasticity to match the line used in the wave tank.

4.2 Optimized damping control

The optimal damping for a single WEC was evaluated for each sea state in a power matrix of 41 sea states by performing a damping sweep in the numerical simulation and picking the damping factor leading to the highest power absorption in this sea state. This damping was then applied by the active PTO and a cylindrical buoy during wave tank tests. The waves energy period of the power matrix ranges from 3.5 s to 9.5 s and the significant wave height start at 0.75 m and goes up to 3.25 m. The sea state $T_e = 3.5$ s/ $H_s = 3.25$ m was not performed, due to the unrealistic steep waves.

4.3 Collaborative damping

Two numerical simulation were performed. The first one is called 'static' as out of the five WECs placed perpendicular to the wave front only one is learnable, while the other were cWECs with latching times of 200 $\frac{Ns}{m}$, 300 $\frac{Ns}{m}$, 400 $\frac{Ns}{m}$ and 500 $\frac{Ns}{m}$. The lWEC uses a 'deep' artificial neural network. In the second run called 'dynamic', two WECs, both learnable, are placed perpendicular to the wave front. The first WEC using exactly the same ANN as in the first test, while the second WEC, uses the more 'shallow' ANN and an exploration function.

The experimental test was performed in a different way: two constant damping WECs were used simultaneously in the wave tank. During the training sequence, sample sets of the winning device for each control period were recorded. This data was used to train the ANN offline. The evaluation was done analougously: The measured force data recorded by the cWECs in the evaluation wave sequence was used offline as input for the lWEC. Its output was then compared to the best constant latching time of the two WECs in the wave tank.

4.4 Collaborative latching

Three different latching strategies were used for the collaborative learning in the numerical simulation: constant latching WECs, of which one is the central WEC without latching, a linear latching WEC and the learnable WEC.

In the simulation four WECs were participating: One central WEC, which also acts as a cWEC with a latching period of 0 s, two cWEC with 3 s and 1.25 s latching time and one lWEC, trained with the same wave sequences as in the CL damping experiments. The evaluation was done with the evaluation wave sequence from the CL damping experiments, but also performing a power matrix consisting of 17 sea states with wave energy periods ranging from $T_e =$ 3.5 s to 9.5 s and with significants wave heights from 0.75 m to 3.75 m; The sea state of $T_e = 3.5$ s / $H_s = 3.75$ m was excluded, due to the unrealistic steep waves. The three strategies compared are the constant latching time of 1.25 s (which performed best of the constant latching times in the evaluation wave sequence), the linear latching and the learnable network. The reference for all this strategy was a non-latching WEC.

In the wave tank test four WECs were participating: One central WEC, two cWECs with 1.25 s and 0.25 s latching time and the lWEC. The specific WEC and the buoy position, named A, B,C and D (see Figure 4.2) has a big influence on the absorbed power: When applying constant damping for all WECs, the absorbed power of WEC D (normally performing the 1.25 s latching time) reaches only 80% and WEC B (normally performing the lWEC) only 98% of the power of WEC A (normally performing the 0.25 s latching time). As differences in the WEC parameters, for example caused by manufacturing to-

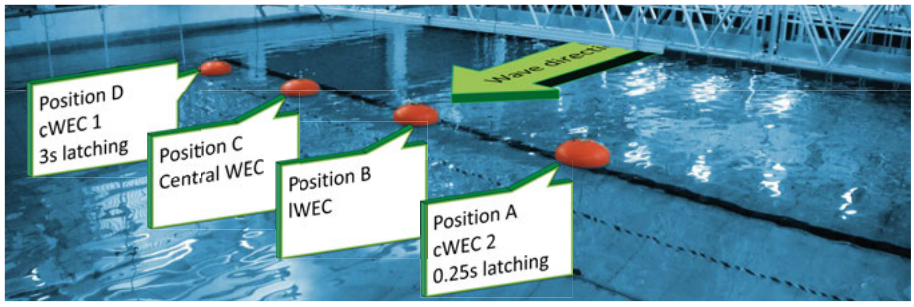

Figure 4.2. Position and applied strategy of the four WECs during the CL latching wave tank test (from Paper V).

lerances or wear, may also occur in real operation, this was not corrected for the CL process. However, it was considered when calculating the absorbed power to get a fair judgement of the different strategies. For the training, the training wave sequence for the wave tank test was used. The evaluation was done with two sea states with $H_s = 1.25$ m and energy period of $T_e = 4.5$ s and $T_e = 7.5$ s.

5. Results

In this section the results are presented, structured in numerical simulation and wave tank tests.

5.1 Optimized natural frequency

The numerically obtained power matrices in Figure 5.1 shows the expected influence of the inertia on the power absorption: Compared to the medium ($M = 45$ t) inertia WEC, the high ($M = 120$ t) inertia WEC absorbs significantly more power in sea states with higher wave periods, while the medium inertia WEC is beneficial for shorter periods. This is especially noticeable for low dampings: here, the maximal absorbed power is much higher than in the case of the high damping factor; On the other hand, for sea states outside the region where wave and WEC are close to resonance the power drops slower with increased damping. The medium inertia WEC, with the high damping, absorbs for all tested sea states more power than the reference WEC. This is not true for the low damping case, where in two cases only 95% of the power output is reached In return the maximal absorbed power for the low damping is 86% higher than the reference, but with the high damping this advantage shrinks to about half (42%). This observation can also be seen in the small power matrix obtained experimentally in Figure 5.2: Here, the high inertia WEC absorbs more power in sea states with long periods and small wave heights, but absorbs less for sea states with short periods and small wave heights. Numerical and experimental test are compared in Figure 5.3. To match simulated an experimental obtained power output, the line elasticity of the wave tank tests has to be modelled into the simulation.

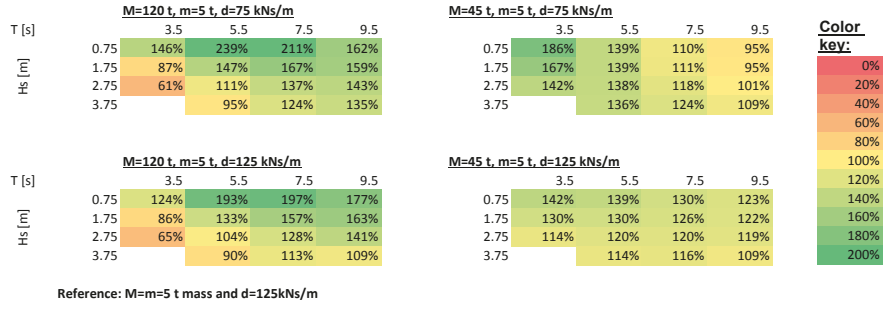

Figure 5.1. Simulated power matrices using two different inertias and damping factors. Reference is a WEC where the mass is equal the inertia (from Paper I).

Power [W], M=53 t, m=5 t, d=100 kNs/m

Hs [m] \ Ts [s]	3.5	5.5	7.5	9.5
0.75	223	626	800	756
1.75	2289	4095	5311	5036

Power [W], M=101 t, m=5 t, d=100 kNs/m

Hs [m] \ Ts [s]	3.5	5.5	7.5	9.5
0.75	155	639	919	915
1.75	1336	2768	4416	4806

Power(M=101 t)/Power(M=53 t)

Hs [m] \ Ts [s]	3.5	5.5	7.5	9.5
0.75	69%	102%	115%	121%
1.75	58%	68%	83%	95%

Color key:

0
1000
2000
3000
4000
5000
6000
50%
80%
110%
140%

Figure 5.2. Experimentally obtained power matrices using two different inertias. The third matrix shows the ratio between the power output of the high and low inertia PTO (slightly modified Figure from Paper I).

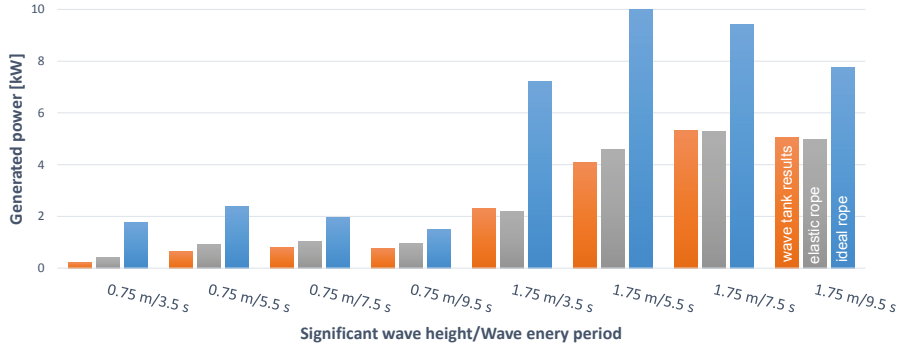

Figure 5.3. Experimentally and numerical obtained power: To get a good agreement, the line elasticity in the simulation has to be lowered. Blue (right) shows the mean power of the simulation using an nearly ideal line, orange (left) shows the mean power from the wave tank tests and grey (middle) the absorbed power of the simulation with the elastic line (from Paper I).

Optimal damping factor for power matrix [kNs/m]

significant wave height [m] \ Energy period [s]	3.5	4.5	5.5	6.5	7.5	8.5	9.5
0.75	60.00	80.00	110.00	140.00	160.00	190.00	210.00
1.25	60.00	80.00	100.00	120.00	140.00	160.00	180.00
1.75	60.00	70.00	90.00	100.00	120.00	140.00	160.00
2.25	50.00	60.00	70.00	90.00	100.00	120.00	130.00
2.75	50.00	60.00	70.00	80.00	90.00	100.00	120.00
3.25		50.00	60.00	70.00	80.00	90.00	110.00

Figure 5.4. Optimal damping factor for each sea state. Obtained with the numerical simulation (from Paper II).

Power matrix (Simulation) [kW]

significant wave height [m] \ Energy period [s]	3.5	4.5	5.5	6.5	7.5	8.5	9.5
0.75	1.71	2.08	2.14	2.06	1.93	1.80	1.67
1.25	4.75	5.77	5.90	5.61	5.26	4.87	4.50
1.75	9.27	11.03	10.92	10.26	9.51	8.80	8.11
2.25	15.07	17.67	16.73	15.51	14.31	13.25	12.18
2.75	21.73	24.00	23.05	21.15	19.50	18.00	16.56
3.25		31.29	29.71	27.17	24.96	23.00	21.13

Figure 5.5. Power matrix from the numerical simulation, using the optimal damping values (from Paper II).

5.2 Optimal damping control

The numerical obtained matrix in Figure 5.4 shows the optimal damping factor for each sea state. It can be seen that the optimal damping increases with the wave energy period but decreases with the wave height. The corresponding power is plotted in Figure 5.1. The absorbed power is increasing with the wave height. Regarding the wave energy period, the maximum depends on the wave height: for significant wave heights equal or higher than $H_s = 1.75$, $T_e = 4.5$ s is the energy period leading to the highest power absorption, while for smaller significant wave heights $T_e = 5.5$ s is optimal. The power matrix obtained in the wave tank shows a much lower energy absorption and the trends are not as clear, see Figure 5.6. However, here it can also be seen that the power increases with the wave height, but a optimal wave energy period can hardly be seen.

5.3 Collaborative Damping

The absorbed power in both test runs of the CL learning in the numerical simulation can be seen in Figure 5.7. In the first test, while using only one learnable WEC, but three cWECs, the learnable WEC absorbs neglectable more power than the constant WECs. However, while having two learnable

Power matrix (wave tank) [kW]

significant wave height [m] \ Energy period [s]	3.5	4.5	5.5	6.5	7.5	8.5	9.5
0.75	0.29	0.73	0.35	0.16	0.10	0.12	0.09
1.25	1.21	1.52	0.68	0.61	0.50	1.67	0.50
1.75	1.58	2.08	1.95	1.66	1.75	2.44	1.31
2.25	1.69	4.60	3.60	1.91	3.25	3.22	2.20
2.75	4.57	5.06	7.35	3.95	3.99	5.64	3.22
3.25		7.40	9.62	4.52	6.83	7.73	6.95

Figure 5.6. Power matrix from the wave tank experiments, using the optimal damping values (from Paper II).

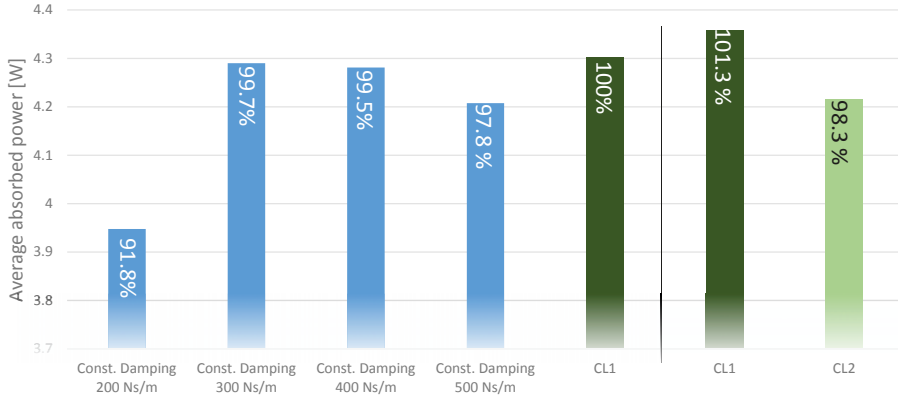

Figure 5.7. Absorbed power during the evaluation wave. The first run was done with four constant damping and one learnable WEC, while the second run was done using two constant dampings and two learnable WECs (from Paper IV).

WECs, the power absorption of the best performing lWEC could be increased to 1.3% more than the best performing constant damping WEC. The second WEC was limited by its exploration function, what explains the lower power absorption.

Figure 5.8 shows how the chosen damping factor of the WEC when fed with the recorded force data from the evaluation wave sequence during the wave tank tests (orange curve). It is compared to actual winning damping factor (so the damping factor leading to the highest power absorption) for each interval (blue curve).

5.4 Collaborative Latching

5.4.1 Numerical Simulation

With help of the numerical simulation the trained policy of the WEC could be examined in detail for the evaluation wave. Figure 5.9 shows the absorbed

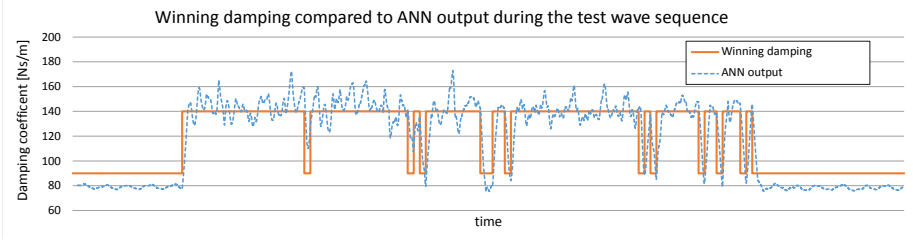

Figure 5.8. Experimentally obtained data was used to train the learnable WEC, which then was fed with the measured input data during the evaluation wave sequence. Orange is the output damping of the learnable WEC, blue the winning damping of the constant WECs (from Paper IV).

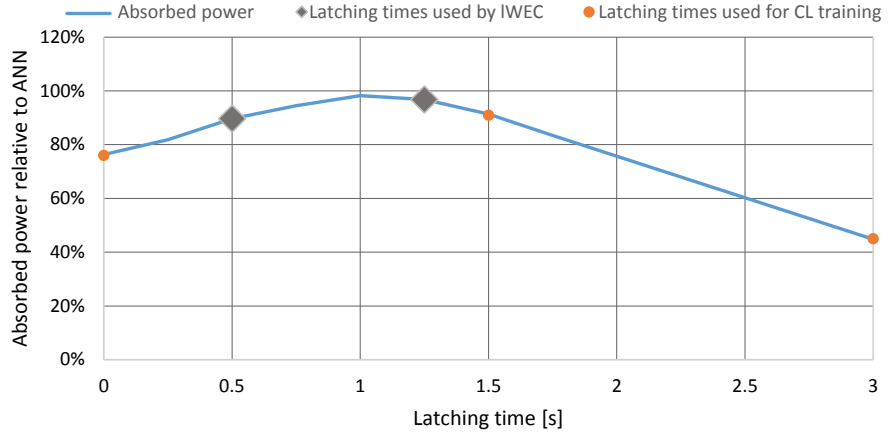

Figure 5.9. In blue the performance of a damping sweep of different latching constant in the evaluation wave is plotted. The absorbed power is set in relation to the absorbed power of the lWEC (100%). The orange dots mark the constant latching times of the cWECs used during learning, while the grey diamonds indicates the latching times the lWEC learned to apply (from Paper V).

power for different constant latching times (blue curve) in relation to the absorbed power by the lWEC. The orange dots indicates the constant latching times that were used during the learning phase and the grey diamonds indicate the latching times applied by the lWEC during the evaluation test sequence. A time series of the latching time absorbing the most power for each latch period during the evaluation sequence is plotted in Figure 5.10 a), while the diagram in b) shows the same data plotted over the mean wave period. In both cases the glowing blue dots indicate the choice of the lWEC.

The lWEC was than compared to the linear latching time in the evaluation wave sequence, see Figure 5.11. The chosen latching time, marked as circles is plotted over the mean wave period. The radius of each circles corresponds to the absorbed power, a yellow dot inside the circle indicates that this latching

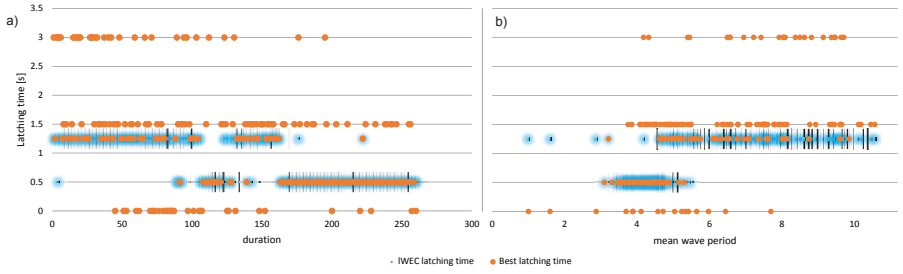

Figure 5.10. The orange dots mark the latching time that absorbed the most power during a latch period in the evaluation wave. In a) the data is plotted over the duration of the wave sequence, while in b) the same data is plotted over the mean wave period. The glowing blue dots indicates the chosen latching time of the lWEC (from Paper V).

time absorbed most power for this wave. The data obtained from the run with the linear latching time had to be matched with the run of the lWEC. Due to the different radiated waves, both runs differ slightly, resulting in small errors while matching both time series, causing that a few points of the linear latching time are outside the line.

The lWEC, the cWEC which absorbed the most power in the evaluation wave (1.25 s latching) and the linear WEC were than used to simulate 15 sea states to form a small power matrix in Figure 5.12. They were all compared to a WEC without latching, but otherwise same characteristics.

5.4.2 Experimental wave tank tests

Instead of the evaluation wave sequence two sea states with different wave energy periods ($T_e = 4.5$ s and $T_e = 7.5$ s; $H_s = 1.26$ m for both) are used for the wave tank test evaluation. The results in the absorbed power for all three strategies in each sea states as well as the total absorbed power is plotted in Figure 5.13. The values are referenced to the mean value of each category. The short latching time absorbed about 6% more power in the $T_e = 4.5$ s sea state, and 4% less in the $T_e = 7.5$ s sea state compared to the long latching time. For the total absorbed power, both constant latching times absorb the same amount of power, because during the $T_e = 7.5$ s sea state more power is absorbed than in the $T_e = 4.5$ s sea state.

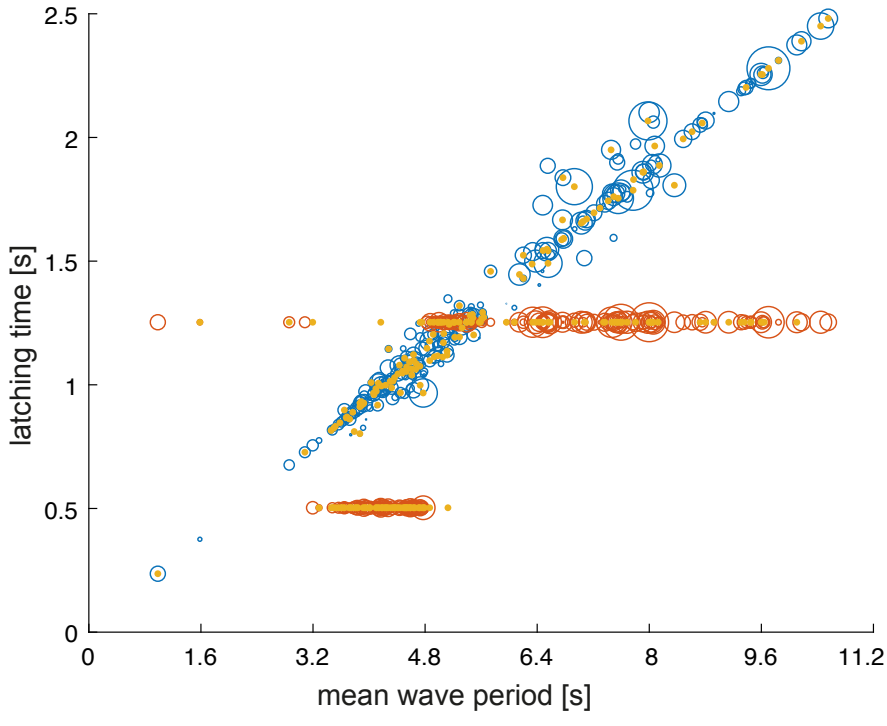

Figure 5.11. Chosen latching times of the lWEC (orange) and the linear WEC (blue) during the evaluation wave plotted over the mean wave period. The radius of the circles correspond to the absorbed power, while a yellow dot indicates which latching time was beneficial for the specific latch period (from Paper V).

a)

Hs [m] \ Te [s]	3.5	5.5	7.5	9.5
0.75	111%	188%	195%	182%
1.75	88%	135%	156%	160%
2.75	71%	109%	127%	138%
3.75		103%	118%	123%

b)

Hs [m] \ Te [s]	3.5	5.5	7.5	9.5
0.75	147%	186%	224%	235%
1.75	119%	133%	163%	182%
2.75	101%	111%	126%	147%
3.75		104%	117%	126%

c)

Hs [m] \ Te [s]	3.5	5.5	7.5	9.5
0.75	142%	178%	217%	215%
1.75	113%	137%	162%	177%
2.75	91%	116%	127%	143%
3.75		106%	116%	125%

Reference: identical WEC without latching

a) Constant latch time: 1.25 seconds
b) Linear latching time
c) CL-ANN

Figure 5.12. Power matrices of a WEC with 0.25 s constant latching time, linear latching time WEC and the lWEC (from Paper V).

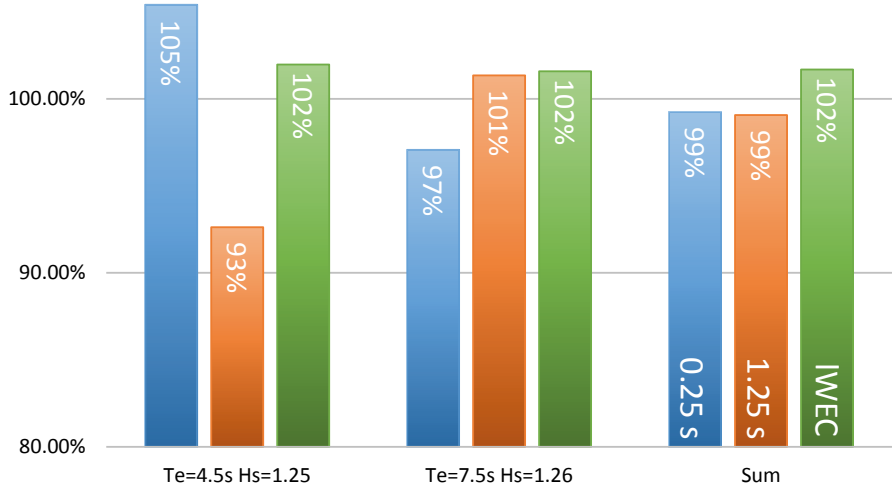

Figure 5.13. Absorbed power during the wave tank test of the lWEC and two WECs with constant latching times of 0.25 s and 1.25 s. The results are plotted for the two different sea states, as well as the total absorbed power during both sea states. The reference for each sea state is the mean absorbed power of all three strategies in this sea state (from Paper V).

6. Discussion

6.1 Optimized natural frequency

In both the numerical results in Figure 5.1 and the experimental results in Figure 5.2 it can be seen that a higher inertia can increase the power absorption significantly. For the simulated power matrix in Figure 5.1 the power absorption is up to two times higher compared to a device without added inertia. The four power matrices show furthermore, how well the absorption characteristic of the device can be tuned with the inertia and the damping factor: The latter has a big influence on the capture bandwidth, while with the inertia the WEC can be tuned for a specific wave period. In contrast to the consideration on the single body WEC in section 2.2.1, the wave height has a significant influence on the absorbed power: When the line is slack, buoy and translator/rotor can move independent and so both will have different oscillation frequencies as when the line is tensioned.

The large differences between Figure 5.2 and 5.1 are explained with the line elasticity and the elasticity introduced by the structure guiding the rope (see Figure 5.3).

6.2 Optimal damping control

The power absorption in the simulation in Figure 5.5 is approximately 5 times higher than what was measured during the wave tank experiments (see Figure 5.6). Reasons for this are

- Friction in the generator as a result of a not ideally centred load was present during all tests, leading to deformation of the translator and so to a non-uniformly distributed friction. This could be partly compensated with a force opposing the friction and post processing Kalman filtering.
- The generator needs some time to ramp down the generator force, which results in similar effects as static friction
- The elasticity of the line may have played a role as the results of the optimal natural frequency tests have shown in Figure 5.3.

Especially the friction may explain why the influence of the energy period is not as clear in Figure 5.6 as it in in Figure 5.5. During the wave tank test, the equilibrium position of the translator, which shifted slightly between the tests, mostly because the line was lengthening in the beginning, had a significant

influence on the absorbed power: If the equilibrium position was on a part with high friction the force to move the translator was significantly higher than on a position with low friction. The influence of the wave height however can be clearly seen in both Figures.

Remarkable about the optimal damping distribution (Figure 5.4) is, that the damping varies much more for the lower than for the higher significant wave height: For $H_s = 0.75$ m the highest damping is 3.5 higher than the lowest damping, while in the $H_s = 2.75$ m this ratio shrinks to 2.5. The absorbed power (from the simulation) however, changes only by 2.4% for the lower wave height, but by 31.3% for the higher one. Since the absorbed power is approximately 15 times higher for $H_s = 2.75$ than for $H_s = 0.75$, it may be suitable for real WECs to focus on sea states with higher significant wave heights when adjusting their damping.

6.3 Collaborative Learning

Comparing experimental results of both, damping and latching, CL strategies Figure 5.7 and 5.13, it can be seen that the lWEC hardly absorbs more than the best cWEC. For the collaborative damping (Figure 5.7) it can be seen, that the damping factor has only a very low influence on the power absorption: While the highest damping factor is 2.5 time the lowest, the power absorption between the extremes differs only by 8.6 %. Under this aspect, even a small increase in the power absorption of the CL lWEC of up to 1.6 % compare to the best cWEC is remarkable.

For the different latching times, the differences in the absorbed power in the evaluation sequence (see Figure 5.9) are in general more obvious: In the tested range from 0 s to 3 s latching time, the absorbed power varies by more than 50%. But even here is the advantage of the lWEC over the cWEC with about 2% very small. Plotting the absorbed power of the lWEC for several sea states, as done in the power matrix in Figure 5.12, the advantage of the lWEC strategy becomes clearly visible: Compared to the 1.25 s cWEC, the lWEC is beneficial in 12 out of 15 sea state (with one draw), and absorbs up to 30 % more power, while the cWEC absorbs at most 6% more power. Using the total absorbed power during the evaluations sequence is only a weak indicator for the quality of a control. The results of both CL strategies suggest let assume that also it consists of a wide range of sea states, at the end there is one dominating latching time/damping factor, reducing the visibility of the adaptive control advantage.

6.3.1 lWEC compared to linear latching time

A special focus should be put on how the lWEC is choosing its latching time. Therefore it is compared with the linear latching time WEC. Figure 5.11 plots

the chosen latching time for both strategies. The lWEC uses just two latching times: Between a mean wave period of 3.2 s and 4.8 s it is most likely that a latching time of 0.5 s is chosen, while for all other cases the 1.5 s latching time is more lickely. An explanation of this strategy is given in the following:

- ANNs are separating problems via (hyper)planes, making them inefficient for linear regression.
- The chosen latching time are nearly always lower than the latching times chosen by the lWEC. A longer latching time may result in a higher absorption if the prediction is correct or the wave has a longer period than predicted. But it may result in a much lower or no power absorption if the wave is shorter than predicted. So a smaller latching time can be seen as a conservative approach. The highest power absorption of all waves can be seen for the linear latching time, however, these are only a few latching periods. For most latching periods, the power absorption between the strategies is more or less equal.
- For mean wave periods below 3.2 s the high latching time is chosen, what is contrary to the conservative approach claimed above. Two explanation for this behaviour should be given: a) the available training data for mean wave periods below 3.2 s could be too less to train the network correctly; b) the WEC can only absorb insignificant amount of power from waves below 3.2 s, it therefore concentrates on waves with higher period that may occur inbetween these waves.

As can be seen in the power matrix in Figure 5.12, the differences in absorbed power between lWEC and linear latching WEC are small: Also the linear latching WEC absorbs more power in 12 of the 15 sea states, the benefits are small (between 0.6% and 11%).

6.3.2 Wave tank tests

As can be seen in Figure 5.13 the lWEC is in each sea state 2% better than the average of all WECs it was learning from. Comparing it in the $T_e = 7.5$ s/ $H_s = 1.25$ m case with the $t_l = 1.25$ s cWEC, the benefit of the lWEC is with 1% significantly smaller than in the same sea state of the numerical simulation (3%, see the power matrix in Figure 5.12). This might be caused by the larger buoy in the wave tank experiments, but also by the imperfect latching of the active PTO, which lowers the advantage of latching in general: In both sea states the difference between 0.25 s and 1.25 s latching times is just about 4%. In relation to this even the 3% advantage in power absorption over both cWECs is significant.

From Figure 5.8 it can be seen that the the ANN used to learn to distinguish between both damping factors. However, it usually prefers the higher damping.

7. Conclusion

Four different ways to optimize the power absorption for a WEC were presented, of whom two are designed for arrays of similar devices. Each strategy has its own advantage.

When the PTO inertia and damping factor can be adapted in the design process, the WEC can be tuned to fit a specific sea state. If the wave climate is close to this state, the WEC will be able to have a good capture width also without control and may even detune itself in storms. But due to the non-linear behaviour of the system caused by the slack line the advantage of a high PTO inertia decreases when the wave height increases. During the wave tank test the elasticity of the line caused furthermore a higher optimal wave period than expected.

Changing the generator damping of a converter can be achieved for most WEC designs. The ratio the damping has to change within two wave periods decreases if the significant wave height increases. If the most of the wave energy may be captured with sea states with higher significant wave heights, also the damping factors the WEC has to support can be decreased.

In the collaborative learning, either the oscillation period (by using latching control in CL latching) and the generator damping factor (in CL damping) were adjustable. By evaluating different strategies at the same time it is able to finding suitable control parameter. It therefore needs neither a model of the WEC nor information about the future sea state, but is able to select a suitable control parameter based on easily obtainable data (force sensor data for CL damping and translator position for CL latching). While the absorbed power for the CL damping was the same (‘static’ test) or slightly higher (‘dynamic’ test) than a constant damping factor, the Cl latching was able to increase the power absorption significantly.

8. Future work

The collaborative learning approach tested in this thesis may be extended in several ways. The ANN used for the CL latching that was presented in Paper V uses just the mean wave period as input, also the latching time is wave height dependent as well. Having two inputs would be a small change that could increase the quality of the control a lot. Furthermore the used ANN is very small, using a deep convolution neural network with the surface elevation as time sequence input could lead to an improved ability to forecast the correct optimal latching time. See therefore also [42], where an ANN is used to forecast waves.

An inherent drawback of the CL as presented here, is that it only focuses on WECs in a row and does not consider interaction between WECs at all. But to increase the total power absorption in a farm, the interactions may have a significant influence. While exchanging wave information between rows could simplify the estimation of the best control parameter (see for example [43]) and while considering the influence of control betweens row the power absorption could increase further.

9. Summary of Papers

Paper I

Performance of a Direct-Driven Wave Energy Point Absorber with High Inertia Rotatory Power Take-off

In this manuscript the problem of designing a simple but accurate physical scale PTO model of a direct-driven floating point wave energy converter is addressed, by presenting a new PTO design that is able to absorb in some sea states significantly more power than a direct-driven linear generator. The physical model presented here simulates an alternating rotatory generator, the nearly ideal constant damping of the PTO is achieved by using an eddy current break. The characteristics of this PTO type, especially the high inertia, are examined using numerical simulations and 1:10 wave tank tests.

The author developed the physical PTO and the numerical model, performed the numerical tests and participated in the planning and performing of the physical wave tank test at Plymouth University's COAST lab.

Paper II

Optimal Constant Damping Control of a Point Absorber with Linear Generator In Different Sea States: Comparision of Simulation and Scale Test

A direct driven WEC with sea state optimized damping factor is used in this paper to get a power matrix with 41 sea state. Therefore the optimal damping factor is obtained via a damping sweep in a numerical simulation. The so obtained damping factors are then used in the numerical simulation and in 1:10 scale wave tank tests to get the power matrix.

The author developed the control system for the physical PTO, performed the numerical tests and participated in the planning and performing of the physical wave tank test at Plymouth University's COAST lab.

Presented by the author at the 12th European Wave and Tidal Energy Conference in Cork, Ireland, 2017.

Paper III

Multi-parameter optimization of hybrid arrays point absorber Wave Energy Converters

The paper investigates the optimization of the impact of the presence of different sized WECs in an array. Three different cases and cost functions are investigated. In the first case the optimal WECs sizes (two different possible WEC sizes) for a 6x6 WEC layout were investigated. In the second scenario the WECs were given (6 small ones, 6 large ones) and the best position in a 6x6 grid were searched. In the third scenario, three WEC parameter (buoy radius and draft and PTO damping) were optimized for a 2x2 array. The optimal layouts suggest that WECs of the same type should be ordered in rows parallel to the wave front and that the optimal generator damping relies barley on the position of the WEC in the array.

The author was part of the project team and reviewed the paper.

Paper IV

A model free control based on machine learning for energy converters in an array", Submitted to Big Data And Cognitive Computing

The paper addresses the problem of finding the optimal control parameters for different situations (states) for energy converters working in an array. It therefore presents a new approach using an artificial neural network that learns during operation while observing the control strategies and energy absorption of all converters in the array and by that learning the best strategy for each situation. This approach is evaluated for wave energy converter with the help of a numerical simulation and a physical 1:10 scale test in a wave tank.

The author developed the control system of the physical PTO and the numerical model, performed the numerical tests and participated in the planning and performing of the physical wave tank test at Plymouth University's COAST lab.

Paper V

Experimental and numerical collaborative latching control of wave energy converter arrays

In this paper the problem of robust latching control of wave energy converters (WECs) in irregular sea states is addressed by introducing a model free, machine learning based collaborative learning strategy for wave energy converters in arrays.

This strategy parallelize the machine learning and solves the problem of finding an evaluation function for the learning algorithm. As learnable element a shallow artificial neural network is used. A numerical simulation and a wave

tank test both performed with an array consisting of five WECs showed that the collaborative learning can increase the power absorption compared to a constant latching time WEC and is robust enough to handle the irregularities of the wave tank test.
The author developed the control system for the physical PTO performed the numerical and physical wave tank test. .

10. Svensk sammanfattning

Vågkraft kan bli en viktig del från framtidens elektriska energikälla. Men därför kostnaden per producerat energienheten måste minskas. En väg att minska kostnaden är att förbättra effektiviteten med ett avancerat styrsystem. Den här avhandlingen tester olika kontrollstrategier för att hitta en bra strategi för vågkraftverk i parker. Alla strategier testas med en numerisk simulering och ett fysiskt test med en 1:10 skalmodell i en våg bassäng.

Först är en elektrisk vågkraft konverter (WEC) med optimerad naturlig frekvens men utan styrsystem är testad. WECen absorberar hög effekt i ett litet område med de vanligaste vågklimatet. Storlek på området kan varieras med generatorns dämpning och bästa vågperiod kan ändras med WECens tröghet.

En generator med optimal dämpningsfaktor testas, för att en justerbar generator dämpning är relativt lätt att implementerar. Numerisk simulering visade att optimal dämpningsfaktor beror på vågperiod och minskar när våghöjden ökar. Beroende av effekten från våghöjd kan ses i numerisk simulation och fysiksals test, men beroende av effekten från vågperiod kan ses bara i numerisk simulation.

Därefter, en modell oberoende strategi (som kallas CL) för vågkraftkonverter i arrayer är presenterat och testad för att styra (1) generator dämpningsfaktor och (2) latching tid. Resultat är att den CL kontrollerade generatorn dämpning endast visar små fördelar med absorberat energi. Men med en CL optimerat latching tid, absorberat effekten ökas mer som 100% i vissa vågklimat.

11. Acknowledgement

A big thank you to my main supervisor Jens Engström, who did not always have an easy time supervising me. Than I want to thank my other supervisors, Mikael Eriksson, Jan Isberg and Erland Strömstedt, and of course my supervisor during my visit in Plymouth Martyn Hann and Edward Ransley, who was not officially a supervisor but helped a lot. A "tack so mycket" also to Malin and Marianna from the SUPERFARMS group, it was really nice to work with you in a team. Our IT administrator Thomas had quite often a hard time with my computer, as I had a lot of special requests. He was mostly able to help me quickly, so that my limited user rights were not as catastrophic as I expected in the beginning. Thank you very much Thomas!

The wave tank experiments were always a highlight during my research. Without the help of the COAST lab team, Greg, Andy, Hanna, Alastair and of course Kieran and Peter it would be impossible to have done this experiments. Furthermore Oliver, Liz and Tara helped a lot during our second experiments and Tom assisted during the third experiments and when analysing the data! Thanks Tom for spending your free time to help!

For the possibility to have an extended research visit in Plymouth I want to thank Mats Leijon for his consent, Deborah Greaves for inviting me to Plymouth, the whole team of the School of Engineering, and of course Jesse, Katrina, Nye, Josh, Ashley and especially Anton.

Thanks is also going to my former officemates in Uppsala with Dalina, Aya, Ligou, Flore, Victor and Francisco and my new officemates Anke, Eirini, Nasir and Per.

I want to thank the Swedish Energy Agency (project number 40421-1), the Swedish Research Council (VR, grant number 2015-04657) and the Åforsk Foundation (ref. nr. 16-591) for funding this research. This work was additionally supported by Stand Up for Energy.

References

[1] Alain Clément, Pat McCullen, António Falcão, Antonio Fiorentino, Fred Gardner, Karin Hammarlund, George Lemonis, Tony Lewis, Kim Nielsen, Simona Petroncini, M.-Teresa Pontes, Phillippe Schild, Bengt-Olov Sjöström, Hans Christian Sørensen, and Tom Thorpe. Wave energy in europe: current status and perspectives. *Renewable and Sustainable Energy Reviews*, 6(5):405 – 431, 2002.

[2] Björn Bolund, Erik Segergren, Andreas Solum, Richard Perers, Ludvig Lundström, Adam Lindblom, Karin Thorburn, Mikael Ericsson, Karin Nilsson, Irina Ivanova, O Danielsson, Sandra Eriksson, H Bengtsson, E Sjöstedt, Jan Isberg, Jan Sundberg, Hans Bernhoff, K-E Karlsson, Ane Wolfbrandt, Olov Ågren, and Mats Leijon. Rotating and linear syncronous generators for renewable electric energy conversion : an update of the ongoing research projects at uppsala university. In: *Nordic Workshop on Power and Industrial Electronics, NORPIE, 14-16 juni, 2004, Trondheim, Norway*, 2004.

[3] I Ivanova, O Ågren, H Bernhoff, and M Leijon. Simulation of a 100 kw permanent magnet octagonal linear generator for ocean wave conversion. In: *Fifth European wave energy conference 17-19 Sept*, 2003.

[4] Jens Engström, Rafael Waters, Magnus Stålberg, Erland Strömstedt, Mikael Eriksson, Jan Isberg, U Henfridsson, K Bergman, J Asmussen, and Mats Leijon. Offshore experiments on a direct-driven wave energy converter. In: *Proceedings of the 7th European Wave and Tidal Energy Conference, 11-13 September 2007, Porto, Portugal*, 2007.

[5] Simon Tyrberg, Magnus Stålberg, Kalle Haikonen, Jenny Tedelid, Jan Sundberg, Mats Leijon, Cecilia Boström, Rafael Waters, Olle Svensson, Erland Strömstedt, Andrej Savin, Jens Engström, Olivia Langhamer, and Halvar Gravråkmo. The lysekil wave power project: Status update. In: *Proceedings of the 9th European Wave and Tidal Energy Conference, September 2011, Southampton, UK*, 2011.

[6] Erik Lejerskog, Halvar Gravråkmo, Andreij Savin, Erland Strömstedt, Simon Tyrberg, Kalle Haikonen, Remya Krishna, Cecilia Boström, Magnus Rahm, Rickard Ekström, Olle Svensson, Jens Engström, Boel Ekergård, Antoine Baudoin, Venugopalan Kurupath, Ling Hai, Wei Li, Jan Sundberg, Rafael Waters, and Mats Leijon. Lysekil research site, sweden : A status update. In: *Proceedings of the 9th European Wave and Tidal Energy Conference, Southampton, UK, 2011*.

[7] Yue Hong, Erik Hultman, Valeria Castellucci, Boel Ekergård, Linnea Sjökvist, Deepak Elamalayil Soman, Remya Krishna, Kalle Haikonen, Antoine Baudoin, Liselotte Lindblad, Erik Lejerskog, Daniel Käller, Magnus Rahm, Erland Strömstedt, Cecilia Boström, Rafael Waters, and Mats Leijon. Status update of the wave energy research at uppsala university. In: *Proceedings of the 10th European Wave and Tidal Energy Conference, Aalborg, Denmark, 2013*.

[8] Arvind Parwal, Flore Remouit, Yue Hong, Francisco Francisco, Valeria Castelucci, Ling Hai, Liselotte Ulvgård, Wei Li, Erik Lejerskog, Antoine Baudoin, M Nasir, Maria Angiliki Chatzigiannakou, Kalle Haikonen, Rickard Ekström, C. Boström, Malin Göteman, Rafael Waters, Olle Svensson, Jan Sundberg, Magnus Rahm, Erland Strömstedt, Jens Engström, Andrej Savin, and Mats Leijon. Wave Energy Research at Uppsala University and The Lysekil Research Site, Sweden: A Status Update. In: *Proceedings of the 11th European Wave and Tidal Energy Conference. Nantes, France, September 2015*.

[9] Oskar Danielsson, Mats Leijon, Karin Thorburn, Mikael Eriksson, and Hans Bernhoff. A direct drive wave energy converter : Simulations and experiments. In *Proc of 24th International Conference on Offshore Mechanics & Arctic Engineering :*. American Society of Mechanical Engineers, 2005.

[10] Jens Engström, M Eriksson, Jan Isberg, and Mats Leijon. Wave energy converter with enhanced amplitude response at frequencies coinciding with swedish west coast sea states by use of a supplementary submerged body. *Journal of Applied Physics*, 106:064512 – 064512, 10 2009.

[11] Maria A. Chatzigiannakou, Irina Dolguntseva, and Mats Leijon. Offshore deployment of point absorbing wave energy converters with a direct driven linear generator power take-off at the lysekil test site. In: *33Rd International Conference On Ocean, Offshore And Arctic Engineering, 2014, Vol 9A : Ocean Renewable Energy*, 2014.

[12] Olle Svensson, Erland Strömstedt, Andrej Savin, and Mats Leijon. Sensors and measurements inside the second and third wave energy converter at the lysekil research site. In: *Proceedings of the Ninth European Wave and Tidal Energy, Southampton, UK*, 2011.

[13] Liselotte Lindblad, Antoine Baudoin, and Mats Leijon. Measurement system for wave energy converter - design and implementation. In: *33Rd International Conference On Ocean, Offshore And Arctic Engineering, 2014, Vol 9A : Ocean Renewable Energy*. AMER SOC MECHANICAL ENGINEERS, 2014.

[14] Rickard Ekström, Senad Apelfröjd, and Mats Leijon. Experimental verifications of offshore marine substation for grid-connection of wave energy farm. In: *3rd International Conference on Electric Power and Energy Conversion Systems (EPECS)*, 2013.

[15] Liguo Wang, Jens Engström, Malin Göteman, and Jan Isberg. Constrained optimal control of a point absorber wave energy converter with linear generator. *Journal of Renewable and Sustainable Energy*, 7, 043127, 2015, doi: 10.1063/1.4928677.

[16] Liguo Wang and Jan Isberg. Nonlinear passive control of a wave energy converter subject to constraints in irregular waves. *Energies*, 8(7), 6528-6542, 2015, doi: 10.3390/en8076528.

[17] Malin Göteman, Jens Engström, Mikael Eriksson, Mats Leijon, Martyn Hann, Edward Ransley, and Deborah Greaves. Wave loads on a point-absorbing wave energy device in extreme waves. *Journal of Ocean and Wind Energy*, 2:176–181, 08 2015.

[18] Malin Göteman, Jens Engström, Mikael Eriksson, and Jan Isberg. Fast modeling of large wave energy farms using interaction distance cut-off. *Energies*, 8(12):13741–13757, 2015.

[19] Flore Remouit. *Automation of underwater operations on wave energy converters using remotely operated vehicles*. PhD thesis, Uppsala University, Electricity, 2018.

[20] Anke Bender, Jan Sundberg, and Olivia Langhamer. Environmental effects from wave power devices on local fish and crustacean communities. In *:Proceedings of the the Environmental Interactions of Marine Renewable Energy Technologies Conference / EIMR* 2018.

[21] Weizhi Wang, Minghao Wu, Johannes Palm, and Claes Eskilsson. Estimation of numerical uncertainty in computational fluid dynamics simulations of a passively controlled wave energy converter. 232:71–84, 02 2018.

[22] K. Budal and J. Falnes. Wave power conversion by point absorbers. *Norwegian Maritime research*, 6(2):2–11, 1978.

[23] Duarte Valério, Pedro Beirão, and José Sá da Costa. Optimisation of wave energy extraction with the archimedes wave swing. *Ocean Engineering*, 34(17):2330 – 2344, 2007.

[24] Jørgen Hals, Johannes Falnes, and Torgeir Moan. Constrained optimal control of a heaving buoy wave-energy converter. *Journal of Offshore Mechanics and Arctic Engineering*, 133(1):011401, 2011.

[25] Guang Li and Michael R. Belmont. Model predictive control of sea wave energy converters - part i: A convex approach for the case of a single device. *Renewable Energy*, 69(Supplement C):453 – 463, 2014.

[26] Pedro Beirao, MJGC Mendes, Duarte Valério, and José Sá da Costa. Control of the archimedes wave swing using neural networks. In *Proc. of the 7th European Wave and Tidal Energy Conference*, 2007.

[27] Tim Mundon, A F Murray, and A R Wallace. Toward a biologically inspired, neural control mechanism for multiple degree of freedom wave energy converters. In *Proc. of the 9th European Wave and Tidal Energy Conference, Southampton, United Kingdom*, 2009.

[28] J. Falnes. *Ocean Waves and Oscillating Systems: Linear Interactions Including Wave-Energy Extraction*. Cambridge University Press, 2002.

[29] WAMIT, Inc. *WAMIT User Manual Version 7.0*. 2013.

[30] M. Eriksson, J. Isberg, and M. Leijon. Theory and experiment on an elastically moored cylindrical buoy. *IEEE Journal of Oceanic Engineering*, 31(4):959–963, Oct 2006.

[31] Jørgen Todalshaug, Johannes Falnes, and Torgeir Moan. A comparison of selected strategies for adaptive control of wave energy converters. *Journal of Offshore Mechanics and Arctic Engineering*, 133, 03 2011.

[32] M. Soliman, O. P. Malik, and D. T. Westwick. Multiple model predictive control for wind turbines with doubly fed induction generators. *IEEE Transactions on Sustainable Energy*, 2(3):215–225, July 2011.

[33] T. R. Mundon, A. F. Murray, J. Hallam, and L. N. Patel. *Causal Neural Control of a Latching Ocean Wave Point Absorber*, pages 423–429. Springer Berlin Heidelberg, Berlin, Heidelberg, 2005.

[34] E. Anderlini, D.I.M. Forehand, E. Bannon, and M. Abusara. Reactive control of a wave energy converter using artificial neural networks. *International Journal of Marine Energy*, 19(Supplement C):207 – 220, 2017.

[35] G. Hinton, L. Deng, D. Yu, G. E. Dahl, A. r. Mohamed, N. Jaitly, A. Senior,

V. Vanhoucke, P. Nguyen, T. N. Sainath, and B. Kingsbury. Deep neural networks for acoustic modeling in speech recognition: The shared views of four research groups. *IEEE Signal Processing Magazine*, 29(6):82–97, Nov 2012.

[36] Alex Krizhevsky, Ilya Sutskever, and Geoffrey E Hinton. Imagenet classification with deep convolutional neural networks. In F. Pereira, C. J. C. Burges, L. Bottou, and K. Q. Weinberger, editors, *Advances in Neural Information Processing Systems 25*, pages 1097–1105. Curran Associates, Inc., 2012.

[37] David Silver, Aja Huang, Chris J. Maddison, Arthur Guez, Laurent Sifre, George van den Driessche, Julian Schrittwieser, Ioannis Antonoglou, Veda Panneershelvam, Marc Lanctot, Sander Dieleman, Dominik Grewe, John Nham, Nal Kalchbrenner, Ilya Sutskever, Timothy Lillicrap, Madeleine Leach, Koray Kavukcuoglu, Thore Graepel, and Demis Hassabis. Mastering the game of Go with deep neural networks and tree search. *Nature*, 529(7587):484–489, January 2016.

[38] Chenhua Ni and Xiandong Ma. Prediction of wave power generation using a convolutional neural network with multiple inputs. *Energies*, 11(8):2097, 2018.

[39] Sepp Hochreiter and Jürgen Schmidhuber. Long short-term memory. 9:1735–80, 12 1997.

[40] Volodymyr Mnih, Koray Kavukcuoglu, David Silver, Alex Graves, Ioannis Antonoglou, Daan Wierstra, and Martin Riedmiller. Playing atari with deep reinforcement learning. *arXiv preprint arXiv:1312.5602*, 2013.

[41] Mikael Eriksson, Rafael Waters, Olle Svensson, Jan Isberg, and Mats Leijon. Wave power absorption : Experiments in open sea and simulation. *Journal of Applied Physics*, 102(8):084910–084910–5, 2007.

[42] A. Castro, R. Carballo, G. Iglesias, and J.R. Rabuñal. Performance of artificial neural networks in nearshore wave power prediction. *Applied Soft Computing*, 23:194 – 201, 2014.

[43] Paul-Emile Meunier, H. Alain, Jean-Christophe Gilloteaux, and Sofien Kerkeni. Development of a methodology for collaborative control within a wec array. In *Proc. of the 12th European Wave and Tidal Energy Conference, Cork, Ireland*, 2017.